Title
Mass Spectrometry-based Proteomic Analysis of Oral Cancer Cells

Author
Ji, Eoon Hye

Publication Date
2014

Peer reviewed|Thesis/dissertation

UNIVERSITY OF CALIFORNIA

Los Angeles

Mass Spectrometry-based Proteomic Analysis of Oral Cancer Cells

A thesis submitted in partial satisfaction

of the requirements of the degree Master of Science

in Oral Biology

by

Eoon Hye Ji

2014

ABSTRACT OF THE THESIS

Mass Spectrometry-based Proteomic Analysis of Oral Cancer Cells

by

Eoon Hye Ji

Master of Science in Oral Biology

University of California, Los Angeles, 2014

Professor Shen Hu, Chair

Mass spectrometry (MS), especially tandem mass spectrometry (MS/MS), is a powerful tool for proteomic and metabolomics applications. Untargeted metabolomics results can be well visualized and interpreted by using the cloud plot with XCMS Online software. The first objective of this study is to perform a comprehensive metabolomics analysis of oral cancer cells and identify metabolites altered by the knockdown of either adenylate kinase 2 (AK2) or phosphorylate glycerol kinase 1 (PGK1). UM1 and UM2 oral cancer cells were treated with siRNA to knockdown AK2 or PGK1. MS/MS and XCMS were performed to compare the metabolite profiles between the cells with siRNA knockdown and with scrambled siRNA control. Our studies confirmed the utility of XCMS to interpret the metabolomic results from oral cancer cells. When AK2 or PGK1 was knocked down in the UM1 or UM2 cells, more metabolites were found to be down-regulated than up-regulated. Heat map analysis indicates that a common

group of metabolites were altered by AK2 knockdown between the UM1 and UM2 cells, and similar finding was observed for the PGK1 knockdown study.

Tracer-based metabolomics, a subset of metabolomics with a labeled substrate, is a new platform that would help researchers understand the metabolic phenotype of cancer cells. The second objective of this study is to develop the novel methodology which combines the tracer-based metabolomics, immunoprecipitation (IP), and MS-based proteomics to detect the metabolic labeling of a specific protein from the entire protein complex in oral cancer cells. [U-$^{13}C_6$]-glucose was introduced into the UM1 and UM2 cells, and the labeled proteins were analyzed by liquid chromatography (LC) with MS/MS. We found that UM1 and UM2 cells displayed different types of ^{13}C labeled peptide mass isotopomer distribution patterns. Mass isotopomer distribution pattern decayed faster and the intensities of each isotopic peak were lower for the UM2 cells than those for the UM1 cells. We also demonstrated that a specific labeled protein, e.g., 78kDa glucose-regulated protein (GRP 78), can be pulled down with IP and analyzed by LC-MS/MS. Our results indicated that the UM1 cells utilize more glucose than the UM2 cells possibly to maintain their invasive and metastatic phenotypes. Also, the methodologies were able to identify any single ^{13}C-labeled protein from the whole cell lysate if antibody is commercially available. Therefore, using XCMS and our newly developed tracer-based metabolomics, we may have an improved understanding of the metabolic phenotype of oral cancer cells.

The thesis of Eoon Hye Ji is approved.

Carl Maida

Robert Chiu

Shen Hu, Committee Chair

University of California, Los Angeles

2014

DEDICATION

This work is dedicated to

Dr. Shen Hu for guiding all of my graduate studies,

my family and friends for loving and supporting me throughout my life, and

God for always being by my side.

We thank Dr. Junhua Wang and Dr. Liangliang Sun for their help.

TABLE OF CONTENTS

LIST OF FIGURES

LIST OF TABLE

INTRODUCTION

A. Oral and Head and Neck Cancer

Head and neck tumors occur in the oral cavity, oropharynx, hypopharynx, larynx and mouth. The most common type of head and neck tumor is called oral squamous cell carcinoma (OSCC). OSCC occurs more frequently in male patients than female patients and in patients who have been exposed to tobacco or alcohol usage [1]. In the US, there are approximately 7,900 OSCC deaths among the 39,400 diagnosed cases per year [2]. OSCC is considered as the sixth most common cancer among men. In addition, it is usually detected in lymph nodes due to the metastatic characteristic [3].

In this study, we primarily use two oral cancer cell lines, UM1 and UM2, for proteomic and metabolomic analysis. UM1 and UM2 cell lines were originally established from a pre-treatment patient who had a single tongue carcinoma. The UM1 cells have more invasive potential and higher motility than the UM2 cells [4].

B. Proteomics

Proteomics is a powerful technology for identifying and studying the characteristics, functions and structures of proteins [5]. Proteomics has been involved in many research fields recently due to its ability to analyze protein expression at specific cellular responses both quantitatively and qualitatively. Quantitative proteomics profiles the entire proteins in a sample quantitatively to find the differences between samples, such as in healthy and in diseased patients which help to understand the molecular mechanisms of diseases [6]. Through proteomics, this study identified characteristics of protein from different oral cancer cells.

C. Mass Spectrometry and Tandem Mass Spectrometry

Mass spectrometry (MS), especially and tandem mass spectrometry (MS/MS), are common proteomic tools for protein identification and quantification. MS measures protein mass accurately and gives high resolution separation of fragment ions with a very small quantity of

sample. There are two proteomic approaches to profile protein peptides. ‘Top-down’ approach allows a whole protein to be fragmented in the gas phase and can identify small proteins. A limitation of this approach is in the difficulty in fragmentizing large proteins in the gas phase. ‘Bottom-up’ approach applies MS/MS to identify peptides of proteins digested in solution. Peptides are initially ionized within an ionization chamber and fragmented for MS/MS analysis. These fragments are measured to identify peptides and proteins, often with the aid of database searching programs [7, 8]. In this study, MS or MS/MS is used for metabolomic or proteomic analysis.

D. Mass Spectrometry-based Metabolomics

Metabolomics is a tool to study all metabolites which are extracted from cultured cells or body fluid/tissue samples from patients [9], [10]. In addition, metabolic profiling is a platform to analyze a set of metabolites in a biochemical pathway quantitatively [10]. There have been many disease biomarkers which have been found by metabolomics [11]. MS is a powerful tool for metabolomics analysis. Based on MS spectra, various small molecules such as lipids, sugars and amino acids can be identified with MS. Since MS-based metabolomic analysis provides global metabolic profiles which contain thousands of peaks, how to visualize and interpret MS-based metabolomics data remains challenging. Recent studies have shown that XCMS and METLIN metabolite database are valuable tools for analyzing MS-based metabolomic data [12]. In the first chapter of my thesis, we have demonstrated LC-MS/MS and XCMS for profiling the metabolites of oral cancer cells. This study was focused on developing and confirming MS-based metabolomic methodologies for studying oral cancer cells.

CHAPTER 1: Metabolomic Analysis of Oral Cancer Cells with AK2 or PGK1 Knockdown

Specific Aim: To confirm a utility of LC-MS/MS with XCMS Online software for metabolic profiling of oral cancer cells.

Sub Aim 1: To identify the altered metabolites in the UM1 or UM2 cells by AK2 or PGK1 knockdown.

Sub Aim 2: To investigate whether the UM1 and UM2 cells have common metabolites that are altered by AK2 siRNA or PGK1 siRNA.

AK2 or PGK1 were knocked down by siRNA in the UM1 and UM2 oral cancer cells. Metabolites were extracted and analyzed by LC-MS with XCMS Online software. Cloud plots and heat maps were used to analyze the metabolomics data.

CHAPTER 2: A Novel Methodology to identify ^{13}C labeled proteins in Oral Cancer Cells

Specific Aim: To develop a novel methodology which combines tracer-based metabolomics, IP with MS-based proteomics to detect metabolically labeled proteins from the entire protein complex in oral cancer cells

Sub Aim 1: To identify differential ^{13}C labeled protein expression of the UM1 and UM2 oral cancer cells.

[U-$^{13}C_6$]-glucose was introduced in oral cancer cells. ^{13}C labeled proteins of the UM1 and UM2 cells were analyzed with LC-MS/MS. Mass spectrum of ^{13}C labeled proteins in the UM1 and UM2 cells were compared.

Sub Aim 2: To detect a single ^{13}C labeled protein in the UM1, UM2, UM5 and UM6 oral cancer cells using IP and LC-MS/MS.

IP was conducted on a single ^{13}C labeled protein, GRP 78, in UM1, UM2, UM5 and UM6 cells. The ^{13}C labeled GRP 78 of the UM1 cells was analyzed with LC-MS/MS and protein database search.

CHAPTER 1: Metabolomic Analysis of Oral Cancer Cells with AK2 or PGK1 Knockdown

INTRODUCTION

A. A Online Metabolite Database-METLIN

METLIN is a online metabolite database which consists of over 10,000 distinctive metabolites and gives matching results by comparing its data with MS/MS data [11]. There are two types of METLIN databases. The traditional METLIN database is involved in many steps to analyze untargeted metabolites. Samples are analyzed by MS and bioinformatic software and investigated to search for mass-to-charge (m/z) ratios of the peaks of interest in metabolites. Samples, then, get putative identifications from MS/MS, and these putative identified samples are compared with the METLIN database to get identified manually if they are in the online library. This study uses the new version of METLIN database which automatically matches MS/MS data to the METLIN database allowing for researchers to save time. If the MS/MS data does not have matched identification from the METLIN database, this new version of METLIN database can give characteristic fragments of MS/MS data, which can help to classify the molecule[11].

B. XCMS Online Software

Identifying metabolites requires data visualization tools. Various forms (X) of chromatography mass spectrometry (XCMS) Online software generates a cloud plot which is a new visualization tool that covers the limitations of the other data visualization tools. There are four different types of data visualization tools: principal component analysis (PCA), scatter plots, volcano plots, and heat maps. These tools show data with mathematical variables, intensity of each sample feature, or P-value and fold change [12]. In order to interpret untargeted metabolomic results, a cloud plot can be a new visualization tool that can show various data characteristics, including what the other four visualization tools have shown [11, 12]. In the

cloud plot, the retention time (minutes) of each eluted feature is plotted on the x-axis, and mass-to-charge ratio (m/z) of feature lists are plotted on y-axis [6]. In this study, features were plugged into the cloud plot as circles with different sizes based on the log fold changes of features produced by the Welch t-test. This visualization tool informed a variety of information of features depending on their retention time. XCMS helps to recognize and classify features between samples depending on their relative intensities, which are used for calculating P-values and fold changes [13].

C. Metabolomic Analysis of Oral/Head and Neck Cancer Cells

In our previous studies, the metabolites of oral cancer stem-like cells (CSCs) and non stem cancer cells (NSCCs) were profiled using capillary ion chromatography (Cap IC) with Orbitrap MS [14]. Between CSC and NSCC, Cap IC/MS analysis revealed different isomeric compounds and their expression levels. It also aided in elucidating the relationship between the isomers and glycolysis pathway in the CSCs. Due to the superior resolution and sensitivity of Cap IC, they were able to analyze more than 4000 metabolites in oral/head and neck cancer cells.

D. Metabolic Enzymes

AK2 is an adenylate kinase isoform. Functions of adenylate kinases (AK) include motility, differentiation and mechano-electrical signal transduction of cells. When AK2 is mutated in severe combined immunodeficiencies (SCID) patients, they may become deaf. When AK2 is knocked down in drosophila or zebrafish, it will have aberrant leukocyte development or growth suppression. AK interacts with and regulates glycolytic and glycogenolytic pathways which generate adenosine triphosphate (ATP) [15]. PGK1 is an important glycolytic enzyme in the glycolysis pathway[16]. PGK1 is a hypoxia-inducible factor-1α (HIF-1α) regulated enzyme which plays an important role in tumor growth, progression, metastasis, and invasiveness in cancer

[17]. HIF-1α expression is down-regulated in HNSCC [3]. In oral cancer stem-like cells (CSCs), both HIF-1α and PGK1 expression is down-regulated compared to non-CSCs [18].

An objective of this study is to investigate the role of metabolic enzymes, AK2 and PGK1, in the metabolomes of UM1 and UM2 oral cancer cells, with LC-MS/MS and XCMS. We predict that down-regulating AK2 and PGK1 would reflect the metabolic phenotype changes of the UM1 and UM2 cells. LC-MS/MS and XCMS were performed on the UM1 and UM2 oral cancer cells to identify the global metabolomics changes due to the siRNA knockdown of AK2 or PGK1.

MATERIALS AND METHODS

A. Cell Culture

The OSCC cell lines, UM1 and UM2, were cultured in cell culture media, Dulbecco's modified eagle medium (DMEM) (Invitrogen Life Technologies, Carlsbad, CA), supplemented with 10% Fetal Bovine Serum (FBS) (Gemini Bio-Products, CA) and 1% penicillin/streptomycin (Invitrogen Life Technologies, Carlsbad, CA). The cells were incubated in a CO_2 incubator at 37°C with 5.0% CO_2, and the medium was changed every two days until cells reached 90-95% confluence. Cells were washed three times with Dulbecco's Phosphate-Buffered Saline (DPBS) (Invitrogen Life Technologies, Carlsbad, CA) and harvested.

B. siRNA Knockdown

Transfection with siRNA was performed on the UM1 and UM2 cells using Hilymax transfection reagent (HilyMax, Rockville, MD, USA) for 48 hours in 6-well plates according to the manufacturer's instruction. Double-stranded siRNAs of PGK1 (SC-36215, Santa Cruz Biotech, Santa Cruz, CA, USA), AK2 (SC-38906, Santa Cruz Biotech, Santa Cruz, CA, USA), and non-target control scrambled siRNAs (Santa Cruz Biotech, Santa Cruz, CA, USA) were prepared

separately with a transfection reagent. Cells were transfected with siRNAs. After a 24 hours treatment, the cells were maintained in fresh normal growth media for 48 hours.

C. Western Blotting

Western blotting was used to confirm siRNA transfection on level of proteins in the UM1 and UM2 cells. Equal amounts of each protein samples were separated in NUPAGE Novex 4-12% Bis-Tris gels and transferred to nitrocellulose membrane (Bio-Rad). The membranes were blocked with 5% non-fat milk (Santa Cruz Biotech, Santa Cruz, CA, USA) in Tris-buffered saline and Tween 20 (TBST) for 1 hour. After the blocking step, the membranes were incubated with anti-AK2 (H65, SC-28786, Santa Cruz Biotech, Santa Cruz, CA, USA) or anti-PGK1(Y-12, SC-17943, Santa Cruz Biotech, Santa Cruz, CA, USA) primary antibodies in 2% non-fat milk overnight at 4°C. The membranes were washed with TBST 3 times and were incubated with secondary antibodies (GE Healthcare, Piscataway, NJ, USA) in 5% non-fat milk for 1 hour at room temperature. The ECL Plus Detection Kit (GE Healthcare, Piscataway, NJ, USA) was used to develop the films and detect the signal intensity of the proteins. All experiments were performed in triplicates.

D. Extracted Metabolites

UM1 and UM2 oral cancer cells were washed twice with DPBS and with Milli-Q water once to remove all debris and media prior to quenching cells in liquid nitrogen and freezing at -80^{o}C. Subsequently, metabolites were extracted from cells using ice cold 90% methanol:chloform solvent ratio with 9:1. Extracted metabolites were dried using speed vacuum concentrator centrifuge at 38^{o}C before sending to LC-MS analysis.

E. LC-MS/MS and Data Analysis

Sample analysis was performed by liquid chromatography (LC) using a reversed-phase C18 column (Zorbax C18, Agilent, 5µM, 150 X 0.5 mm diameter column) with a flow rate of 20 µL/min. Electrospray ionization time-of-flight mass spectrometry (Agilent 6520 QTOF) was

performed in a positive mode with water/acetonitrile as mobile phases A/B, each containing 0.1% formic acid to analyze samples. Linear changes in mobile phase B composition with time (0 min, 10% B; 5 min, 10% B; 10 min, 40% B; 65 min, 98 B; 70 min, 98% B) were components of the chosen LC gradient. Samples were washed to reduce possible carryover before analysis.

Data analysis was performed using XCMS Online software with free access at https://xcmsonline.scripps.edu/ using three steps: data upload, parameter selection, and result interpretation (Figure 1). The metabolomics features are represented as ions with a unique m/z and retention time. The metabolomics data resulting directly from XCMS generated the cloud plot[13]. Data analysis was also performed using NetWalker 1.0, a desktop application, which can be download for free from https://netwalkersuite.org/. The MS/MS analysis data of features were quantified to generate heat maps. The heat maps were created with NetWalker 1.0 which were composed of log 2 ratio feature/average condition data with a standard deviation greater than 0.5. Log fold changes were produced by a Welch t-test.

RESULTS

A. Cloud plots of AK2 and PGK1 in the UM1 and UM2 Cells

MS/MS analysis data were uploaded to XCMS to generate the cloud plot, aka, mirror plot. Figure 2 showed two different cloud plots: AK2 in the UM1 cells and PGK1 in UM1 cells. As retention times passed, the numbers of eluted features were increased (Figures 2A and B). As retention time reached 30 minutes, each group eluted about 100 to 160 features ($P \leq 0.01$; fold change ≥ 1.5).

B. Features of Metabolites in Different Oral Cancer Cell Lines

To investigate the numbers of metabolite features in oral cancer cells, the metabolites in the UM1 and UM2 cells were analyzed by QTOF. We detected 4280 metabolic features in the UM1 cells with AK2 knockdown, 3183 metabolic features in the UM2 cells with AK2 knockdown,

4736 metabolic features in the UM1 cells with PGK1 knockdown, and 4212 metabolic features in the UM2 cells with PGK1 knockdown from QTOF with positive mode (Figure 3A). Among the total number of features in each group, we also detected 448 metabolic features in the UM1 cells with AK2 knockdown, 369 metabolic features in the UM2 cells with AK2 knockdown, 585 metabolic features in the UM1 cells with PGK1 knockdown and 417 metabolic features in the UM2 cells with PGK1 knockdown ($P < 0.05$) (Figure 3A). The UM1 cells contained more number of features for both AK2 and PGK1 than the UM2 cells (Figure 3A).

In both the UM1 and UM2 cells, 85 metabolic features with AK2 knockdown were presented ($P < 0.05$) (Figure 3B). In the UM1 cells, 18.97% metabolic features with AK2 knockdown ($P < 0.05$) were the same as 23.04% metabolic features in the UM2 cells with AK2 knockdown ($P < 0.05$). In both the UM1 and UM2 cells, 96 metabolic features with PGK1 knockdown were presented ($P < 0.05$) (Figure 3C). In the UM1 cells, 16.41% metabolic features with PGK1 knockdown were the common metabolic features ($P < 0.05$) as 23.02% metabolic features in the UM2 cells with PGK1 knockdown ($P < 0.05$). The common metabolic features between the UM1 and UM2 cells with either AK2 or PGK1 knockdown were composed of a higher percentage in the UM2 cells than the UM1 cells.

C. Metabolites Down-regulated in Different Knockdown Oral Cancer Cell Lines

To identify the role of the features in oral cancer cells with AK2 knockdown or PGK1 knockdown, fold changes in each knockdown cell line were analyzed after treatment with siRNA. Transfection of the UM1 and UM2 cells using siRNA was confirmed by western blotting. AK2 and PGK1 displayed lower expression in the UM1 cells that were transfected with siRNA knockdown (KD) compared to siRNA control (CTRL) (Figure 4A and B). Among the entire feature list of siAK2 or siPGK1 in the UM1 or UM2 cells ($P < 0.05$), more than half of features from each group were down-regulated after the siRNA treatment (Figure 5A). Both the UM1 and UM2 cells showed more down-regulated common metabolic features with siAK2 and siPGK1

than up-regulated common metabolic features with siAK2 and siPGK1 (Figure 5B). In the UM1 or UM2 cells, 61 to 71 down-regulated common metabolic features with AK2 or PGK1 were found after siRNA treatment (Figure 5B and Table 1). Up-regulated common metabolic features in the UM1 and UM2 cells with siAK2 and siPGK1 were selected if log fold changes of the metabolic features were greater than 1. Down-regulated common metabolic features in the UM1 and UM2 cells with siAK2 and siPGK1 were selected if log fold changes of the features were less than 1. Additionally, the common metabolic features in the UM1 and UM2 cells with siAK2 and siPGK1 showed similar patterns of log fold changes values (data not shown).

D. Heat Maps of Common Metabolic Features between the UM1 and UM2 Cells

To investigate the common metabolic features between the UM1 and UM2 cells with AK2 and PGK1 after siRNA treatment, metabolic features in the UM1 or UM2 cells with AK2 or PGK1 intensities from MS/MS data were selected ($P < 0.05$) and were plugged into NetWalker 1.0, a desktop program. Each row represented a different metabolic feature among the control and knockdown samples in the UM1 and UM2 cell lines. Green color represented a lower expression of metabolic features in the cancer cell line, and red color represented a higher expression of metabolic features in the cancer cell line. If the metabolic feature was not expressed in the cancer cell line, it was represented as a black marker in the heat maps. In the UM1 and UM2 cells, a majority of the metabolic features in the heat map displayed a lower expression in the siAK2 treated cells as compared to the control siRNA (siCTRL) treated cells (Figure 6A). Similarly, expression of siPGK1 metabolic features was lower than siCTRL in both siRNA treated UM1 and UM2 cells (Figure 6B).

DISCUSSION

Identifying metabolites is a major step towards the biological interpretation of data in metabolomic analysis. Due to the vast amount of metabolites present in a biological subject or

the wide dynamic concentration range of the compounds, characterizing the metabolome has been a challenge in many research studies. In order to overcome the difficulties of metabolomics, a MS-based metabolomics with XCMS Online software has been applied in this study to determine metabolites of OSCC.

Oral carcinogenesis arises from benign hyperplasia to dysplasia to carcinoma followed by invasive squamous cell carcinoma [16]. OSCC is developed in a multistep process with genetic mutations and expression changes of many genes involved in oral carcinogenesis [16]. Nowadays, there are many proteomics analysis that focus on investigating gene and protein expression in OSCC to understand pathways of proteins or discover potential biomarkers for diagnosis of the disease. In metabolomic analysis, profiling metabolites of OSCC should allow for the understanding of the characteristics of the OSCC.

To profile the metabolites of OSCC, MS/MS analysis data was utilized to generate cloud plots with XCMS. The numbers of AK2 and PGK1 metabolic features in the UM1 cells had a similar pattern in the UM2 cells. Comparing the numbers metabolic features in the UM1 and the UM2 cells with of AK2 and PGK1, the UM1 cells contained the common metabolic features with AK2 and PGK1 in greater amount than the UM2 cells to maintain invasive and metastatic phenotypes. In the UM1 and UM2 cells, around 16% to 23% each cell shared the same metabolic features with AK2 or PGK1 which indicated that the UM1 and UM2 cells possibly share the common metabolic features with AK2 or PGK1.

After silencing AK2 and PGK1, heat maps were generated to present expression of metabolic features in the UM1 and UM2 cells with AK2 and PGK1. Our studies have demonstrated that about 70% of the common metabolic features were down-regulated after treating the UM1 and UM2 cells with siRNA. This indicated that these common features ($p<0.05$) associated with AK2 knockdown between the UM1 and UM2 cells or associated with PGK1 knockdown between the UM1 and UM2 cells reflect the important metabolic phenotypes

of theUM1 and UM2 cells. These down-regulated features in the UM1-AK2 knockdown or the UM1-PGK1 knockdown may be the metabolites that contribute to the UM1 cells having invasive and metastatic phenotypes.

As Rasola et al. stated, glucose uptake is important for cancer cell to maintain their metabolism [19]. A previous study found that when AK2 was knocked down by siRNA, knockdown AK2 resulted in increasing consumption of glucose and glutamine in UM1 and UM2 cells to maintain glycolysis [20]. In glycolysis, AK2 controls and maintains the balance between adenosine monophosphate (AMP) and ATP[15]. AK2 favors binding tightly to AMP which allows AMP to activate AMP-activated protein kinase (AMPK) and triggers glycolysis. Similarly, PGK1 was found to be over-expressed in breast, ovarian, pancreatic and gastric cancers [21]. Furthermore, over-expression of PGK1 promotes the metastasis in prostate cancer cell [22]. Like AK2, PGK1 plays an important role in glycolysis preventing angiogenesis [16]. Consequently, the common metabolic features of AK2 or PGK1 between the UM1 and UM2 cells may have a crucial role in regulating metabolism which helps increase glucose consumption thereby promoting cell survival and differentiation in UM1 and UM2 oral cancer cells.

As Schulze and Harris stated that profiling metabolites of cancer is difficult using MS because some metabolites were present with overlapping spectral peaks. However, using XCMS after LC-MS/MS data analysis, metabolites were separated more clearly without overlapping metabolites because XCMS is more sensitive in detecting small molecules [23]. In LC/MS data, single-quadrupole mass are often detected with wider peak than in XCMS data which can produce a fraction of a mass unit as small as 0.1m/z wide. XCMS can be used to align molecule peaks with retention time. The alignment procedure helps to eliminate insignificant groups of peaks [24]. Eliminating these low resolution groups and incomplete signals using retention time alignment step, samples are only selected with the highest intensity

and have well-behaved peak groups which have potential chance to be matched into sample groups more precisely than in LC-MS/MS analysis [24]. In this study, after silencing AK2 or PGK1 in the UM1 and UM2 oral cancer cells, metabolites of the UM1 and UM2 cells were analyzed and classified with different phenotypes on heat maps using XCMS with LC-MS/MS data. Our data suggest that AK2 and PGK1 correspond to certain metabolic features of the UM1 and UM2 oral cancer cells.

CONCLUSION

Many research studies are conducted to detect thousands of metabolites using MS/MS analysis; however, identifying these metabolites with many visualization tools can be difficult. Profiling metabolites using LC-MS/MS with XCMS is a powerful methodology to combine the benefits of all other visualization tools to identify these metabolites. We have confirmed the utility of XCMS to interpret the metabolomic results from oral cancer cell lines. When AK2 or PGK1 was knocked down in the UM1 or UM2 cells, more metabolites were found to be down-regulated than up-regulated. Heat map analysis indicates that a common group of metabolites were altered by AK2 knockdown between the UM1 and UM2 cells, and similar finding was observed for the PGK1 knockdown study.

CHAPTER 2: A Novel Methodology to identify ^{13}C labeled proteins in Oral Cancer Cells

INTRODUCTION

A. Glucose Metabolism in Healthy Cells and Cancer Cells

Glucose is a crucial element for many organisms to have normal physiological functions. Glucose is used as the energy source for a variety of cellular processes. Normal cells or non-proliferating cells consume glucose and generate pyruvate to produce about 36 adenosine triphosphate (ATP) molecules when oxygen is present. In absence of oxygen, normal cells or non-proliferating cells undergo anaerobic glycolysis in which pyruvate is converted into lactate to produce 2 ATP. However, Otto Warburg discovered that cancer cells or proliferating cells uptake glucose and produces only one pyruvate which generates about 4 ATP whether or not oxygen is present. This glucose metabolism in cancer cells or proliferating cells is called aerobic glycolysis or the Warburg effect [25]. Cancer cells favor uptaking more glucose than normal cells to generate more ATP [26]. Due to a distinctive glucose consumption between normal and cancer cells, we utilize [U-$^{13}C_6$]-glucose as a tracer to study head and neck cancer cells.

B. Tracer-Based Metabolomics

Metabolomics determines small molecules in a biological system. Tracer-based metabolomics, a subset of metabolomics with a labeled substrate, is often used to analyze small molecules and characterize metabolic phenotypes of cells. Radioactive and non-radioactive isotopes, such as ^{14}C from [U-^{14}C]-glucose, have been used for metabolomics with chemical degradation or purification of the product. However, recent studies focus on the use of stable isotopes, such as [U-$^{13}C_6$]-glucose, for tracer-based metabolomics without degradation or purification of the products. The distribution of ^{13}C from a labeled precursor among various metabolic intermediates identifies quantitative relationship between precursor and product in tracer-based metabolomics. The distribution of ^{13}C determines a metabolic phenotypic feature of

the product and the metabolic pathways of the product [27]. The metabolic intermediates are determined by stable isotope tracers and mass isotopomer analysis [28]. Since carbon, nitrogen and hydrogen atoms are incorporated from their precursor substrates through exchanges during the process of amino acid synthesis, a ^{13}C labeled substrate can be involved in metabolites and protein synthesis. Amino acids that are incorporated with a ^{13}C labeled substrate are heavier than “natural” amino acids because they contain more than one isotope. Protein synthesis with a ^{13}C labeled substrate therefore results in a mass shift [29]. Previous studies have been used [U-$^{13}C_6$]-glucose as a single tracer to study on one-carbon metabolism in yeast and bacteria [28]. In this study, the tracer-based metabolomics with a ^{13}C labeled substrate has been applied to studying metabolic phenotypes of oral cancer cells.

C. IP with MS

IP is a common technique for verifying protein-protein interactions of a target protein. In order to identify and purify the target protein from the entire protein complex, a specific antibody is required to bind to the target protein with IP. Studying a single protein can help with understanding of the role of a protein in cellular function and the relationship with the protein and other proteins in a signaling network [30].

In this study, we have developed a novel methodology which introduces [U-$^{13}C_6$]-glucose into oral cancer cells prior to performing IP and MS analysis in order to detect a specific labeled protein. This study aims to demonstrate the following results. First, due to the different characteristics between the UM1 and the UM2 oral cancer cells, ^{13}C labeled peptide mass isotopomer distribution patterns would be different. Second, enrichment of ^{13}C labeled peptides might be higher in the UM1 cells than the UM2 cells. Third, by employing the new protocol, purified ^{13}C labeled 78k Da glucose-regulated protein (GRP 78) would be able to be pulled down by IP and subsequently analyzed by MS. Thus, this new methodology allows researchers to study the biosynthesis of any individual proteins if an antibody is commercially available.

MATERIALS AND METHODS

A. Cell Culture

The OSCC cell lines, UM1 and UM2 were cultured in cell culture media, Dulbecco's modified eagle medium (DMEM) (Invitrogen Life Technologies, Carlsbad, CA), supplemented with 4.5g/L [U-$^{13}C_{6,}$ 99%] D-glucose (Cambridage Isotope Laboratories, Inc.), 10% Fetal Bovine Serum (FBS) (Gemini Bio-Products, CA) and 1% penicillin/streptomycin (Invitrogen Life Technologies, Carlsbad, CA). The cells were incubated in a CO_2 incubator at 37°C with 5.0% CO_2, and the medium was changed every two days for 5 days. When the cells reached 90-95% confluence, the cells were washed three times with Dulbecco's Phosphate-Buffered Saline (DPBS) (Invitrogen Life Technologies, Carlsbad, CA) and harvested.

B. In-solution Trypsin Digestion

Cells were lysed with 8M urea. Each cell lysate obtained equal amounts of total proteins were treated with 200 mM dithiothreitol (DTT) for an hour at room temperature to hydrolyze disulfide bonds. After DTT treatment, protein samples were incubated an hour at room temperature in dark with 150 mM iodoacetamide (IAA) in 200mM ammonium bicarbonate (NH4HCO3) to stabilize the broken disulfide bonds. Samples were, then, incubated with 13.3% w/v solution of trichloroacetic acid (TCA) in acetone to precipitate most proteins at -20°C for 24 hours. The protein pellets were incubated with 10 ng/ul enzyme-grade trypsin (Promega, Madison, WI) in 200mM NH4HCO3 at 37°C for 24 hours to digest proteins. After protein digestion, samples were dried using a speed vacuum concentrator centrifuge at 38°C to remove organic solvents and dissolved in 0.1% of formic acid.

C. IP

Sulfo-NHSb-SS-Biotin (Thermo Scientific, Rockford, IL, USA) with 10mM was incubated with GRP 78 (GTX 62592, GeneTex, Irvine, CA, USA) antibody for 2 hours at room temperature to prepare biotinylated antibody. In order to couple the antibody to the beads, 1 mg/ml of

Dynabeads Myone Strepavidin T1 (Invitrogen Life Technologies, Carlsbad, CA) were incubated with the biotinylated antibody and Dulbecco's Phosphate-Buffered Saline (DPBS) (Invitrogen Life Technologies, Carlsbad, CA) for 30 minutes at room temperature. After incubation, the coated beads were washed twice with DPBS (Invitrogen Life Technologies, Carlsbad, CA) and washed once with 0.01% of bovine serum albumin (BSA). The coated beads were incubated in 0.01% of BSA for 15 minutes at room temperature and washed three times with DPBS. Samples were added into the coated beads and washed with DPBS for three times. Supernatant was removed from the coated beads and 30uL of 0.1M citric acid (pH 2.9) were added into the coated beads to elute the proteins from the coated beads.

D. LC-MS/MS and Database Search

Sample analysis was performed by liquid chromatography (LC) using a reversed-phase C18 column (Zorbax C18, Agilent, 5µM, 150 X 0.5 mm diameter column) with a flow rate of 20 µL/min. Electrospray ionization time-of-flight mass spectrometry (Agilent 6520 QTOF) was performed in a positive mode with water/acetonitrile as mobile phases A/B, each containing 0.1% formic acid to analyze samples. Linear changes in mobile phase B composition with time (0 min, 10% B; 5 min, 10% B; 10 min, 40% B; 65 min, 98 B; 70 min, 98% B) were components of the chosen LC gradient. Samples were run at 180 minute gradient. Samples were washed to reduce possible carryover before analysis. Database searching was performed using Mascot database search engine. Peptide mass isotopomer distribution patterns were manually selected for data analysis.

E. Data Analysis of ^{13}C Labeled Peptides

Xcalibur 2.1 software (Thermo Scientific, Rockford, IL, USA) was used to verify the MS/MS spectra of ^{13}C labeled peptides manually within 380.00-1800.00 m/z range. The highest peak among other isotopic peaks in a mass isotopomer distribution was selected for identifying the sequence of the ^{13}C labeled protein. Peptide fragment b and y ions were used to verify

sequence of protein through SwissProt, a freely accessible resource database of protein sequence.

RESULTS

A. Identification of ^{13}C Labeling in Oral Cancer Cells

In order to test the new methodology to identify ^{13}C labeled protein in oral cancer cells, [U-$^{13}C_6$]-glucose was introduced in the oral cancer cells, UM1 and UM2, through cell culture. The labeled proteins were then collected for LC-MS/MS analysis. From MS1 full scan (380.00-1800.00 m/z), ^{13}C labeled peptide mass isotopomer distribution patterns were manually selected (Figures 7-1A&B, 7-2A&B, 7-3A&B, 8-1A&B, 8-2A&B, 8-3A&B, 9-1A&B, 9-2A&B, 9-3A&B, 10-1A&B, 10-2A&B). As can be seen from the mass spectra, ^{13}C labeled peptide isotopomer distributions displayed decay patterns. The decay patterns were depicted by mass shift which was determined between two isotopic peaks of peptide as 1 dalton (Da).

There were different ^{13}C labeled peptide mass isotopomer distribution patterns, which were constantly observed in many proteins of both the UM1 and UM2 cells. As shown in Figures 7-1C, 7-2C, 7-3C, the first isotopic peak (monoisotopic-base peak, M0, ^{12}C) of the peptide had the highest intensities (relative abundance) among the other peaks. The second isotopic peak (^{13}C labeled peak, M1, ^{13}C) and the third isotopic peak (M2) of peptide displayed lower relative abundance than the first isotopic peak. Between the first and fourth isotopic peaks of peptide, the mass shift was 3 Da. At the fourth isotopic peak of peptide (M3), there was a spike followed by the decay pattern with more than 6 peaks (M4, M5, M6, M7, M8, M9).

The second ^{13}C labeled peptide mass isotopomer distribution pattern displayed a constant isotopic decay pattern (Figures 8-1C, 8-2C, 8-3). This pattern started with the first isotopic peak of peptide as the highest intensities and contained more than five peaks. The third ^{13}C labeled peptide mass isotopomer distribution pattern (Figure 9-1C, 9-2C, 9-3C) was a

similar decay pattern as the first pattern except fourth istotopic peak was the highest isotopic peak among other isotopic peaks. Typically, this type of mass isotopomer distribution pattern consisted of more than 12 consecutive isotopic peaks. Since this type of mass isotopomer distribution pattern had a greater amount of isotopic peaks, more isotopic peaks with high values of intensities than other types of mass isotopomer distribution patterns were observed. The fourth type of ^{13}C labeled peptide mass isotopomer distribution pattern was observed with a greater number of isotopic peaks (Figures 10-1C, 10-2C). The decay pattern contained a spike at the sixth or seventh isotopic peaks and had a concave down decay pattern with numerous consecutive isotopic peaks of consecutive isotopic peaks.

Overall, most of the peptide mass isotopomer distribution patterns displayed higher intensities of isotopic peaks with the UM1 cells when compared to the UM2 cells, and isotopic patterns decayed in a more rapid fashion in the UM2 cells than in the UM1 cells.

B. Confirmation of Purified ^{13}C Labeled 78k Da Glucose-Regulated Protein in Oral Cancer Cells

Western blot analysis was performed to confirm that purified ^{13}C labeled GRP 78 was eluted by IP and purified from unspecific protein in all four oral cancer cells, UM1, UM2, UM5, and UM6 (Figure 11). The expression of ^{13}C labeled GRP 78 in the UM1, UM2, UM5, and UM6 cells were observed with different levels. In the UM1 and UM5 cells, ^{13}C labeled GRP 78 was detected less than in the UM2 and UM6 cells.

C. Identification of ^{13}C Labeled 78k Da Glucose-Regulated Protein in Oral Cancer Cells

^{13}C labeled GRP 78 eluted by IP was analyzed using LC-MS/MS to test whether the new protocol can identify a specific labeled protein. A peptide isotopomer distribution pattern was observed in ^{13}C labeled GRP 78 (Figure 12-1). In ^{13}C labeled GRP 78 mass spectrum, a double envelope pattern containing two peptide isotopomer distribution patterns was detected. The first peptide isotopomer distribution pattern contained a higher spike at the fourth isotopic peak

compared to the first isotopic peak to reflect the double envelope pattern for peptide sequence K.TFAPEEISAMVLTK.M of GRP 78 in the UM1 cells (Figure 12-2). The second peptide isotopomer distribution pattern displayed a consistently decaying pattern with peptide sequence R.ITPSYVAFTPEGER.L of GRP 78 in the UM1 cells (Figure 12-2).

DISCUSSION

Proteins are essential biomolecules for tumor cells to proliferate. There are many studies that identified and analyzed proteins in cancer cells globally using various proteomic tools. Isotopic labeling of protein samples is a common methodology to quantify proteins. Chemical labeling and metabolic labeling are two well-known types of isotopic labeling techniques that most researchers have used. However, these two types of techniques have some limitations. Chemical labeling techniques are often inaccurate and cause errors in peptide modifications. Metabolic labeling technologies employ a stable isotope labeled amino acids which are used for cell culture medium. There are three disadvantages of metabolic labeling: at least two weeks are required for cell culturing with isotope labeling media, cells have a low tolerance to the isotope labeling media, and isotope labeling chemicals are expensive [30].

In this study, we have demonstrated a tracer-based metabolomics methodology for studying oral cancer cells by using [U-$^{13}C_6$]-glucose as a tracer. With this tracer, ^{12}C labeled peptides were replaced with ^{13}C labeled peptides, which may reflect the metabolic path of glucose in the oral cancer cells. Because^{13}C from glucose was converted into the amino acids of proteins in the cells, mass shifts of the peptides derived from proteins were observed in the mass spectra obtained by MS [29]. Since high enrichment of ^{13}C labeling (99%) was used for this LC-MS/MS analysis, all the mass isotopomer distribution patterns should contain ^{13}C labeled peptides in each isotopic peak. Even though a natural abundance of ^{13}C atom is 1.1%, the intensities of many second isotopic peaks (^{13}C) were as high as the first peak (the

monoisotopic peak with ^{12}C because the peptides were labeled with 99% enrichment of ^{13}C. Consequently, each isotopic peak represented the amount of ^{13}C enrichment of each peptide. .

To validate the new methodology, we compared the mass spectra of ^{13}C labeled peptides of the UM1 cells were compared with those of the UM2 cells. Both ^{13}C labeled protein peptides of the UM1 cells and UM2 cells displayed different types of ^{13}C labeled peptide mass isotopomer distribution patterns. Mass isotopomer distribution pattern decayed faster and the intensities of each isotopic peak were lower for the UM2 cells when compared to the UM1 cells. The quantitation of the intensity of each isotopic peak implied that the UM1 cells, which had greater amounts and higher intensities of isotopic peaks than the UM2 cells, consumed more [U-$^{13}C_6$]-glucose than the UM2 cells. In a previous study, the UM1 cells were shown to uptake more glucose for cell proliferation than the UM2 cells based on a glucose uptake assay [20].

On the mass spectra of ^{13}C labeled peptides of the UM1 and UM2 cells, all peptide mass isotopomer distribution patterns displayed with a decay pattern. Each isotopic peak represents relative abundance and ^{13}C enrichment. When an isotopic peak has a higher intensity or relative abundance than other isotopic peaks, that isotopic peak is labeled with ^{13}C more than lower intensity isotopic peak. As m/z increases heavy isotopes occur in the same ionic fragment. Having all heavy isotopes in the same ionic fragment is extremely low probability. Thus, as m/z increases, the peptide has less chance to have all heavy isotope molecules to be labeled and display decay pattern of isotopomer distribution. We also observed many isotopomer patterns had a spike in the fourth isotopic peak. The spike in the fourth peak represents an abundance of ^{13}C incorporated in the isomer. From first peak to fourth peak, there is a 3 Da mass shift. As glucose is utilized by the cell, it is converted into a 3 carbon molecule named pyruvate. Pyruvate is then processed into 3 carbon amino acids such as alanine or serine. As the cell utilizes these newly synthesized amino acids, certain proteins will have a 3 Da shift corresponding to the

heavier amino acids, resulting in a spike on the fourth peak. This may suggest labeling of a 3 carbon amino acid such as alanine or serine in this type of peptide distribution pattern [31].

Relative glucose consumption was correlated with invasive and metastatic phenotype of cancer cells since glucose uptake is used for cell proliferation. Glucose uptake may contribute to the more invasive and metastatic phenotype of UM1 cells than the UM2 cells. Therefore, our study has led to a novel tracer-based metabolomics methodology which can be used to explore the relationship between glucose uptake and the characteristics of cancer cells. This methodology may be also used for identifying the role of a specific labeled amino acid in protein synthesis of oral cancer cells. In a previous study, ^{13}C labeled glucose was used to label multiple positions (C_1, C_2, C_3, C_4, C_5, C_6) of the same molecule to determine its roles of the molecule in glycogen synthesis, gluconeogenesis and tricarboxylic acid (TCA) cycle metabolism [28]. In oral cancer studies, ^{13}C labeled anthrocyanin was used to focus on its synthetic route [32]. Our methodology may also be used to elucidate the role of each amino acid in protein synthesis of oral cancer cells.

In a previous study, a similar methodology combined tracer-based metabolomics and MS-based proteomics was demonstrated for analysis of cancer cells. Although this methodology was feasible for the global analysis of proteins, it was not suitable for targeted protein analysis. In order to overcome the limitation to study on a single protein, we have demonstrated a new methodology by combining IP with LC-MS/MS for targeted analysis of GRP 78 protein.

In this methodology, IP was used to pull down ^{13}C labeled GRP 78 in oral cancer cells to allow for detection by MS. Western blot analysis confirmed that ^{13}C labeled GRP 78 in the UM1, UM2, UM5, and UM6 cells was purified through IP. In the UM1 and UM5 cells, ^{13}C labeled GRP 78 expression was lower than in the UM2 and UM6 cells. Further investigation may address the relationship between GRP 78 and the UM1 or UM5 cells which have more invasive and metastatic phenotypes than the UM2 and UM6 cells. Due to such a small amount of purified ^{13}C

labeled GRP 78 eluted from IP, micro BCA protein assay was not able to measure the GRP 78 concentration in the cells.

Afterwards, LC-MS/MS was used to analyze the peptide isotopomers derived from the eluted GRP 78. Based on database searching against the SwissProt protein database, the peptide sequences were matched and identified and the peptide isotopomer patterns were revealed. Also, comparison of the ^{13}C labeled GRP 78 mass spectra with those of natural GRP 78 indicates that the methodology is valid to isolate and analyze individual ^{13}C labeled protein [20].

Despite successfully proving the global and targeted analysis of proteins in cancer cells with these novel methodologies, there still remain potential limitations. We will be able to study a target protein with this new targeted methodology, only when commercial antibody is available. Tracer-based metabolomics with [U-$^{13}C_6$] glucose can only be applied to studying certain proteins that utilize glucose for their synthesis. In order to study the synthesis and metabolism of other proteins, we will have to use other labeled substrate.

CONCLUSION

We have demonstrated tracer-based metabolomics methodology for global and targeted analysis of proteins in oral cancer cells. Overall, the results from this study suggest that stable isotope tracers can help to elucidate the metabolism of oral cancers related with glucose uptake and protein synthesis. We also found highly invasive UM1 cells utilize more glucose than low invasive UM2 cells possibly to maintain their invasive and metastatic phenotypes. Employing these new methodologies to study proteomics and metabolomics can help discover potential biomarkers in human disease for clinical and diagnostic applications. Moreover, studying protein metabolisms with these methodologies may help reveal targets for therapeutic interventions.

FIGURES

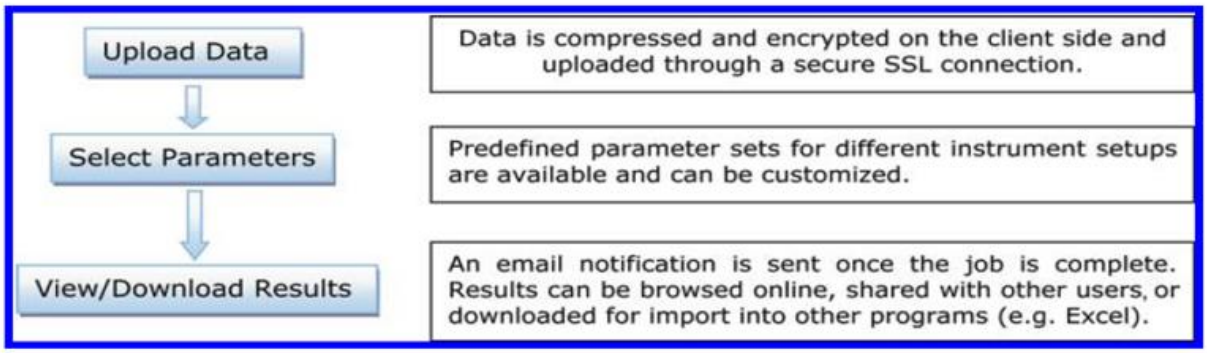

***Figure adopted from Tautenhahn et al., 2012**

Figure 1. XCMS Online software Workflow: MS/MS data is analyzed through XCMS with three steps; uploading data, selecting parameters, and viewing/downloading results.

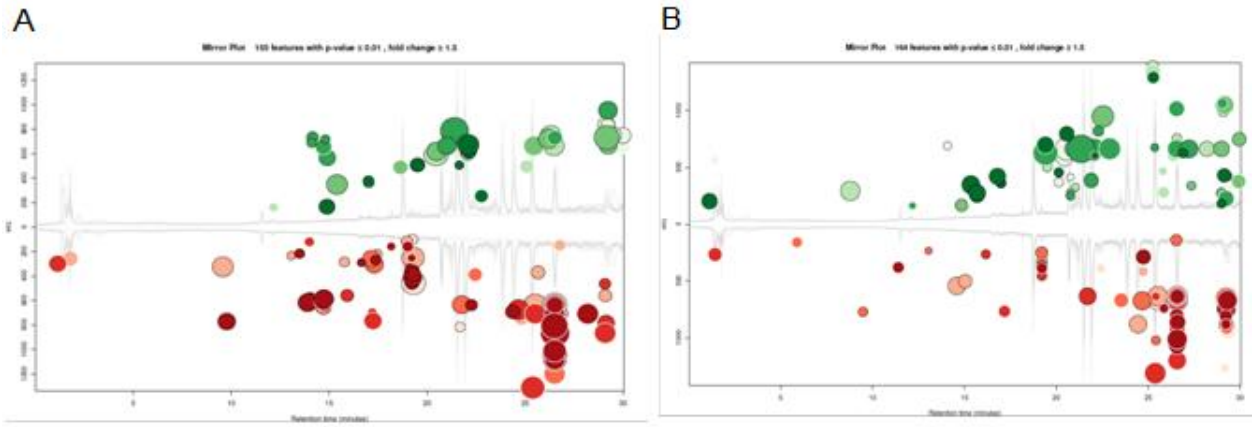

Figure 2. Cloud plots of the metabolites in the UM1 and UM2 cells with siAK2 or siPGK1 knockdown. (A) Cloud plot of the metabolites in the UM1 oral cancer cells with siAK2 knockdown. (B) Cloud plot of the metabolites in the UM1 oral cancer cells with siPGK1 knockdown. The retention times (minutes) of each eluted feature was plotted on the x-axis, and mass-to-charge ratio (m/z) of feature lists were plotted on y-axis[13]. Features were plugged into the cloud plot as circles with different sizes based on the log fold changes of features produced by the Welch t-test. When any of the features had database hits in the METLIN database, the surface of features were displayed with black outlines.

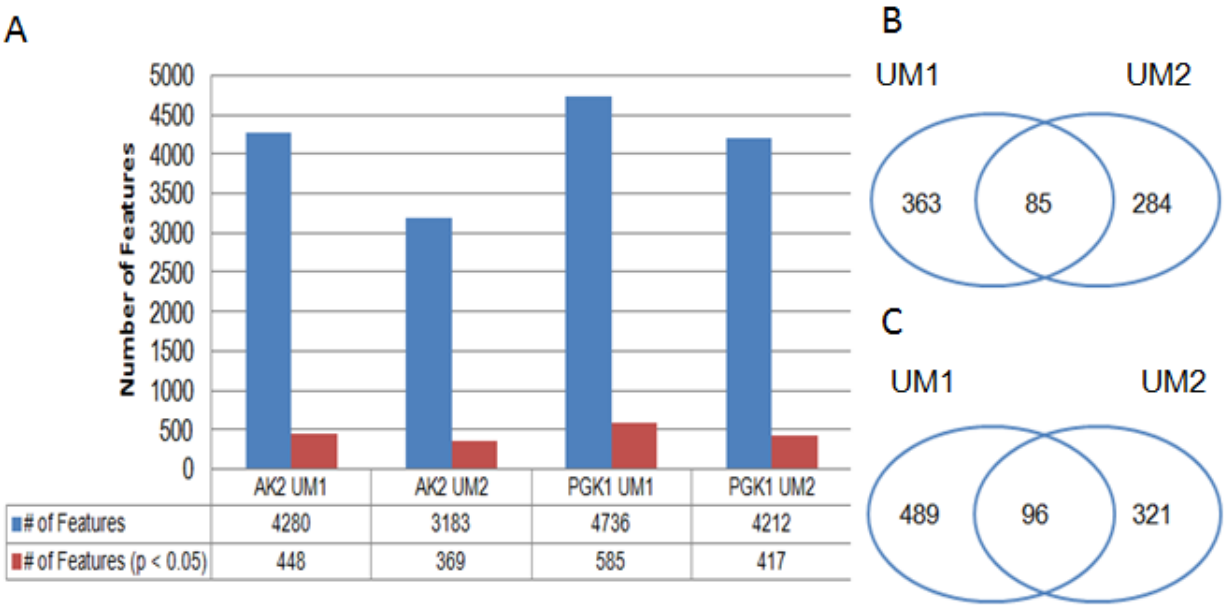

Figure 3. Metabolic features in different oral cancer cell lines. (A) Number of metabolic features detected in the UM1 or UM2 oral cancer cells with either siAK2 or siPGK1 knockdown (entire list or P-value < 0.05. (B) Common metabolic features between the UM1 and UM2 oral cancer cells when AK2 was knocked down. (C) Common metabolic features between UM1 and UM2 oral cancer cells when PGK1 was knocked down.

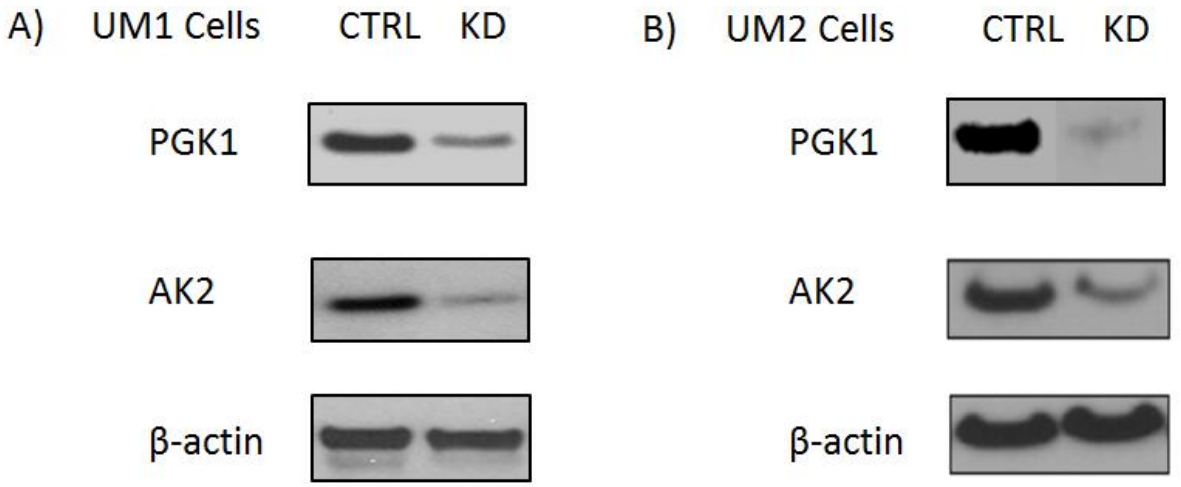

*Figure4 B (AK2) adopted from Chai., 2013.

Figure 4. AK2 and PGK1 protein expression in the UM1 and UM2 oral cancer cells with siRNA knockdown. (A) Western blot data of AK2 and PGK1 protein expression in UM1cells transfected with siRNA control (CTRL) or siRNA knockdown (siAK2 or siPGK1). (B) Western blot data of AK2 and PGK1 protein expression in the UM2 cells transfected with siCTRL, siAK2 or siPGK1.

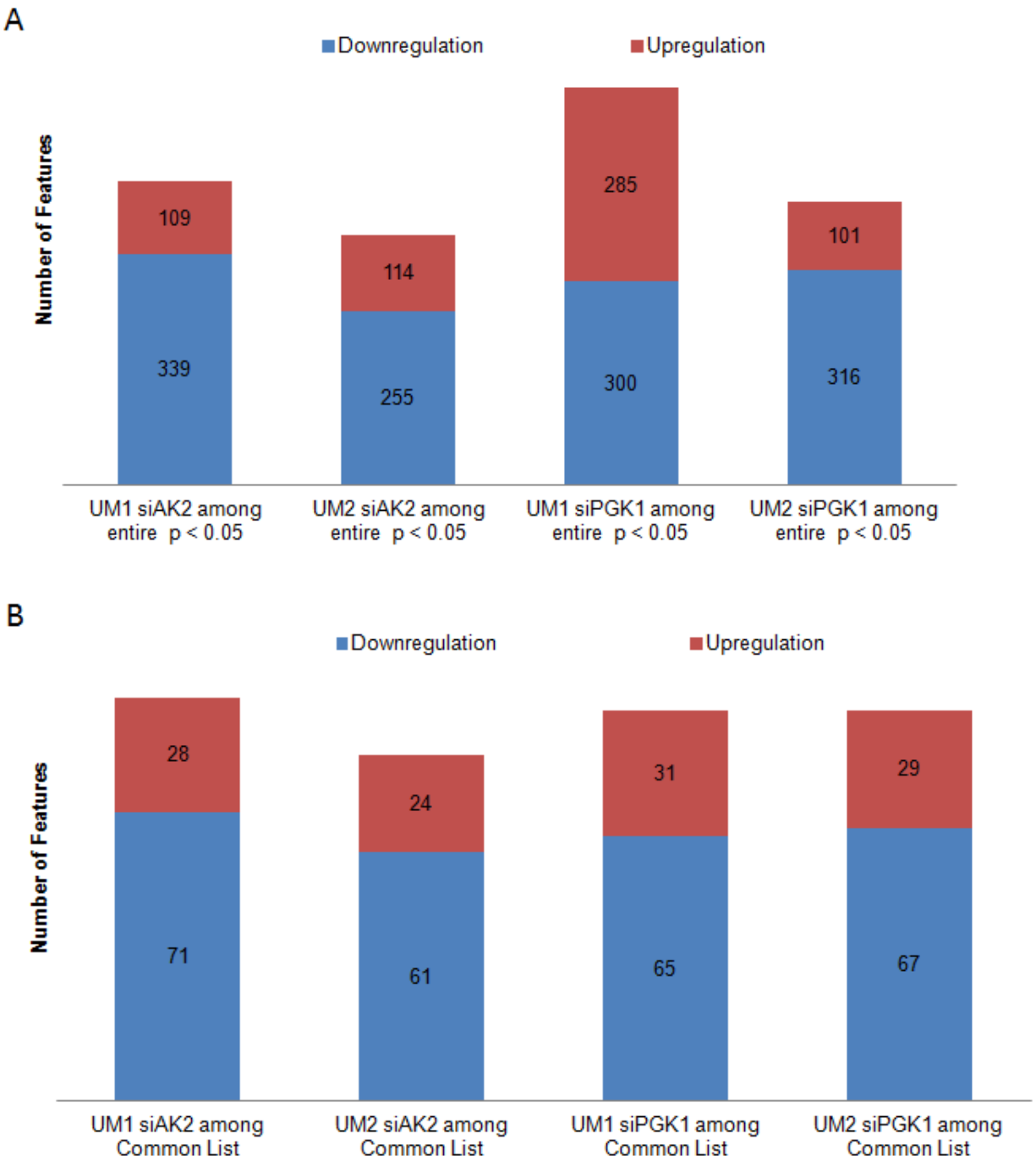

Figure 5. Metabolic features down-regulated in UM1 or UM2 oral cancer cells when AK2 or PGK1 was knocked down. (A) Up or down-regulated metabolic features ($P < 0.05$) in the UM1 or UM2 oral cancer cells when AK2 or PGK1 was knocked down. (B) Up or down-regulated metabolic features ($P < 0.05$) which are common between UM1 and UM2 oral cancer cells when AK2 or PGK1 was knocked down.

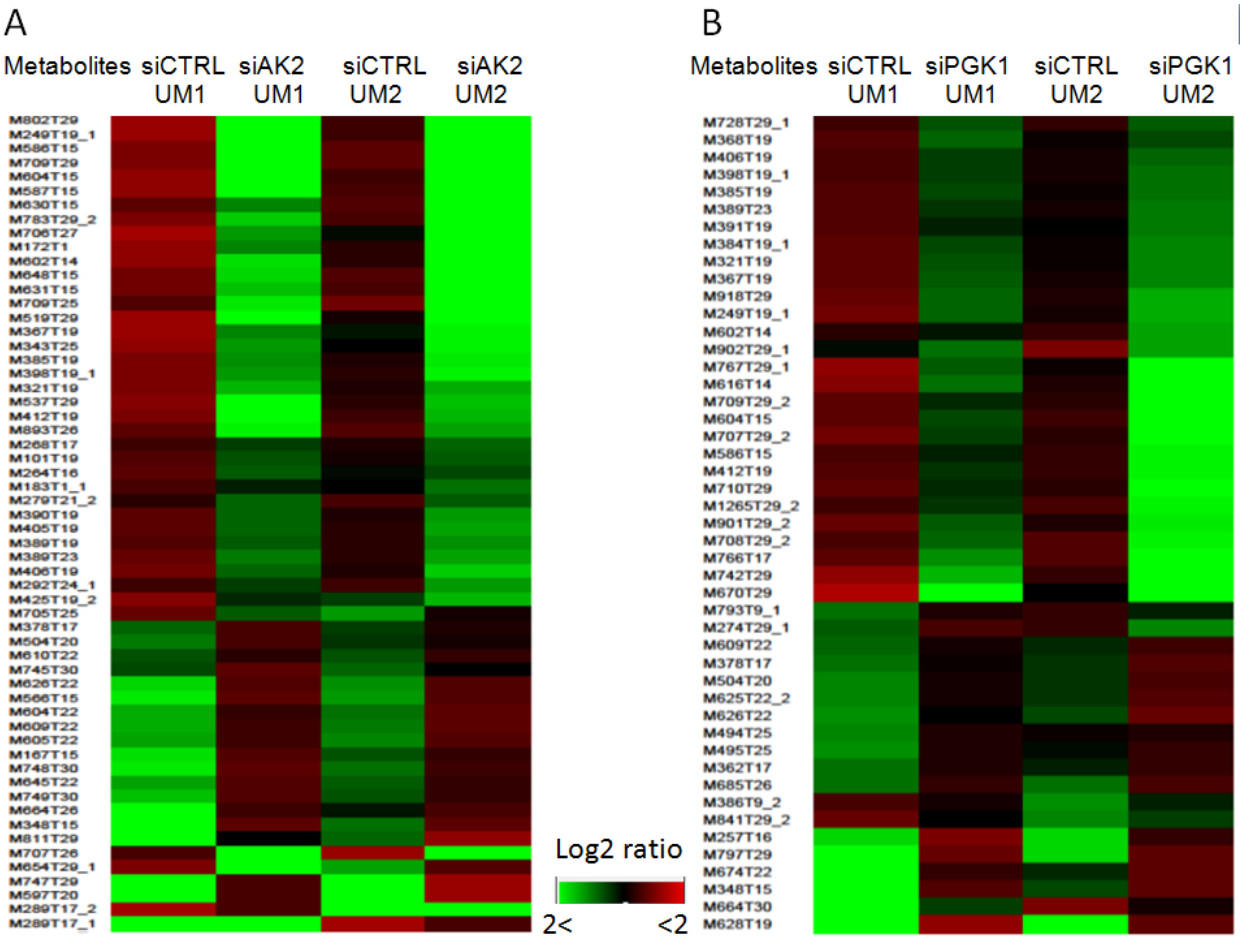

Figure 6. Heat maps with common metabolic features between UM1 and UM2 oral cancer cells. (A) Expression of common metabolites between UM1-siAK2 and UM2-siAK2 cells. (B) Expression of common metabolites between UM1-siPGK1 and UM2-siPGK1 cells.

A.

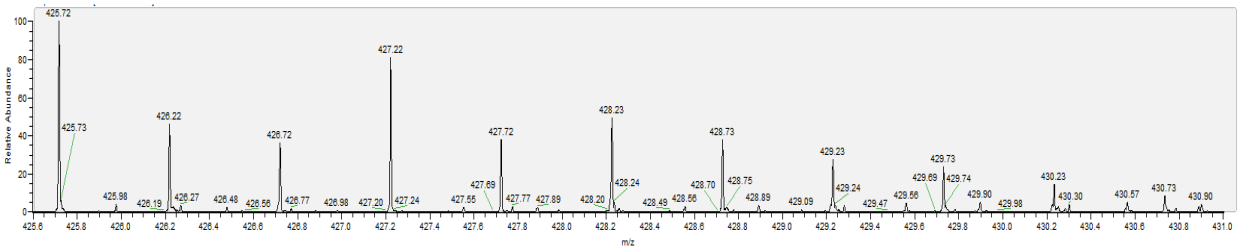

B.

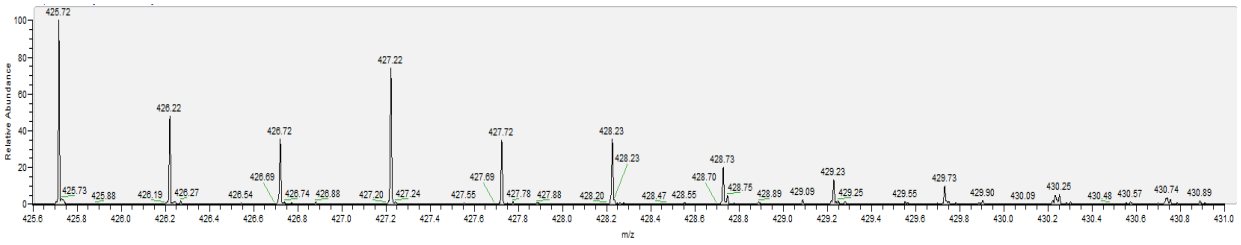

C.

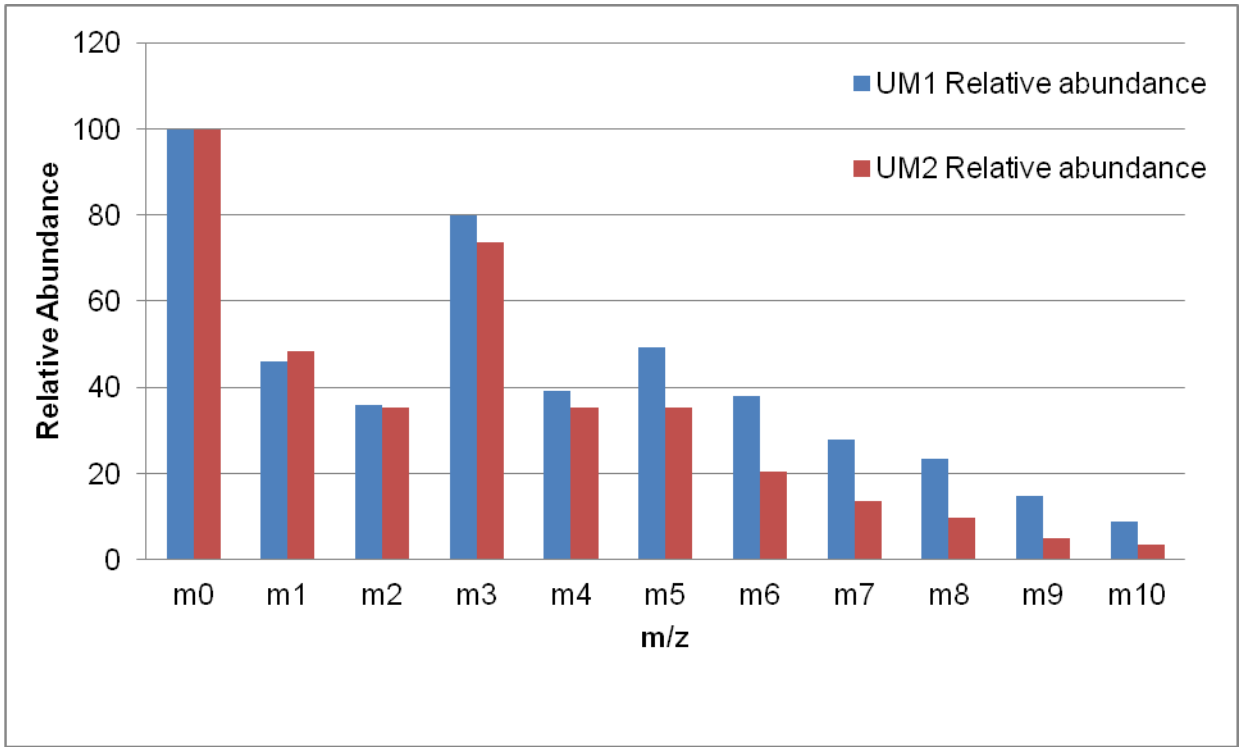

Figure 7- 1. LC-MS analysis of ^{13}C labeled peptide isotopomers in the UM1 and UM2 oral cancer cells (A) ^{13}C labeled peptide mass isotopomer distribution in UM1 oral cancer cells. (B) ^{13}C labeled peptide mass isotopomer distribution in UM2 oral cancer cells. (C) Comparison of relative abundance for ^{13}C labeled peptide mass isotopomer distribution in UM1 and UM2 oral cancer cells.

A.

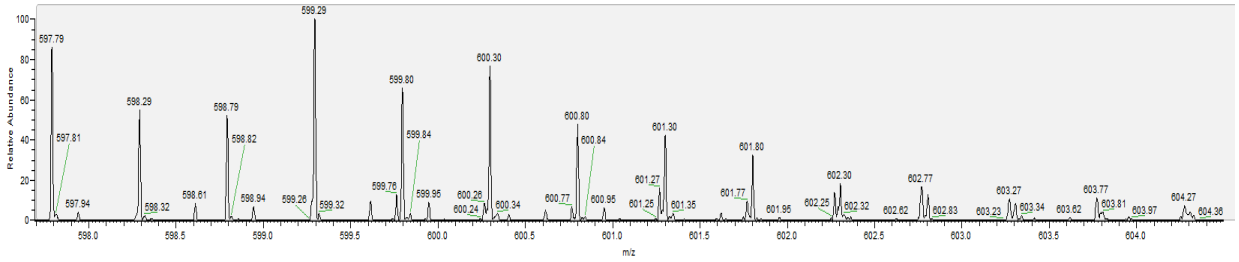

B.

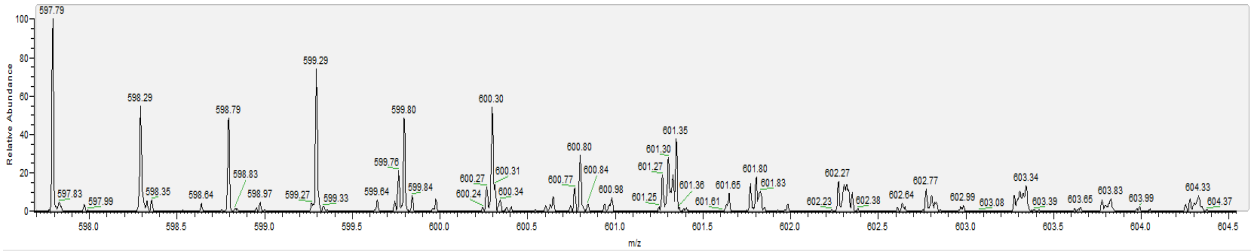

C.

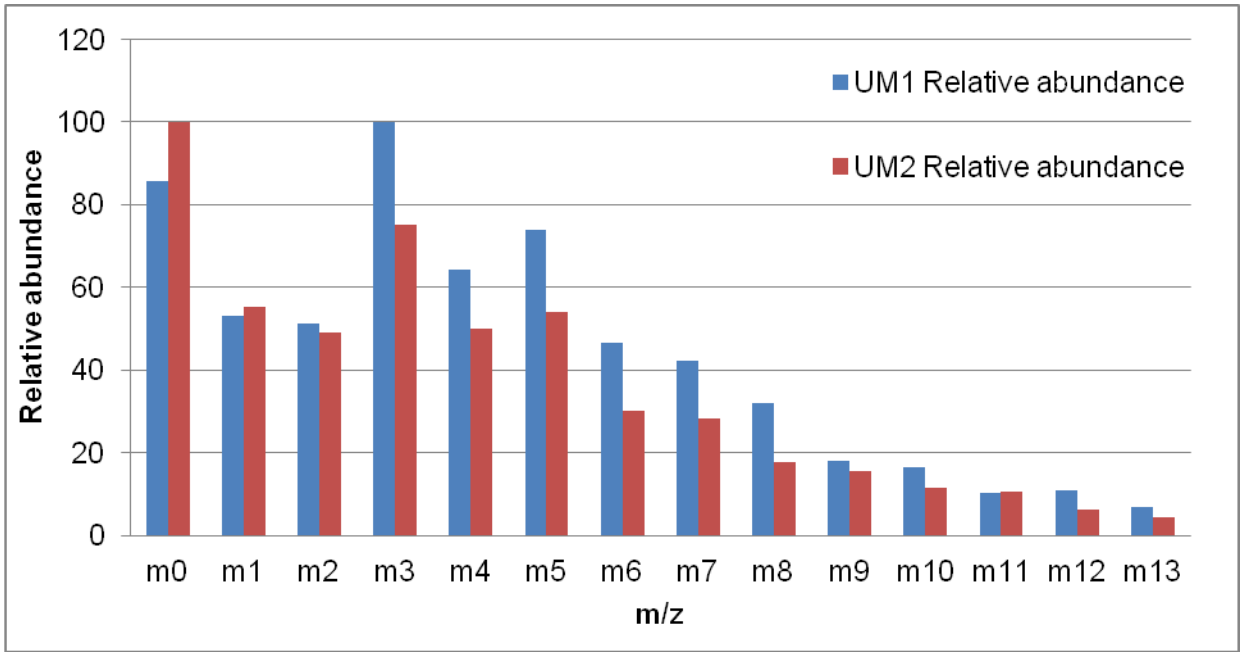

Figure 7- 2. LC-MS analysis of ^{13}C labeled peptide isotopomers in the UM1 and UM2 oral cancer cells (A) ^{13}C labeled peptide mass isotopomer distribution in UM1 oral cancer cells. (B) ^{13}C labeled peptide mass isotopomer distribution in UM2 oral cancer cells. (C) Comparison of relative abundance for ^{13}C labeled peptide mass isotopomer distribution in UM1 and UM2 oral cancer cells.

A.

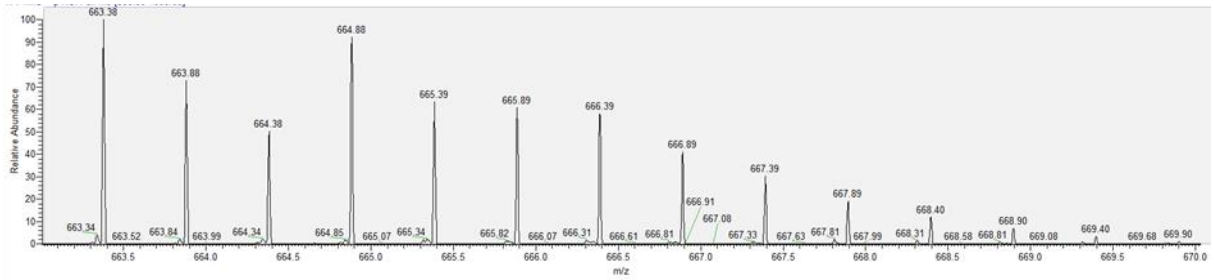

B.

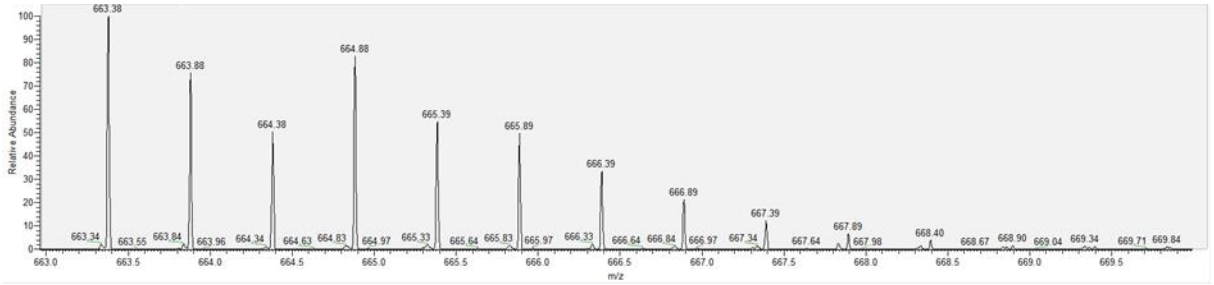

C.

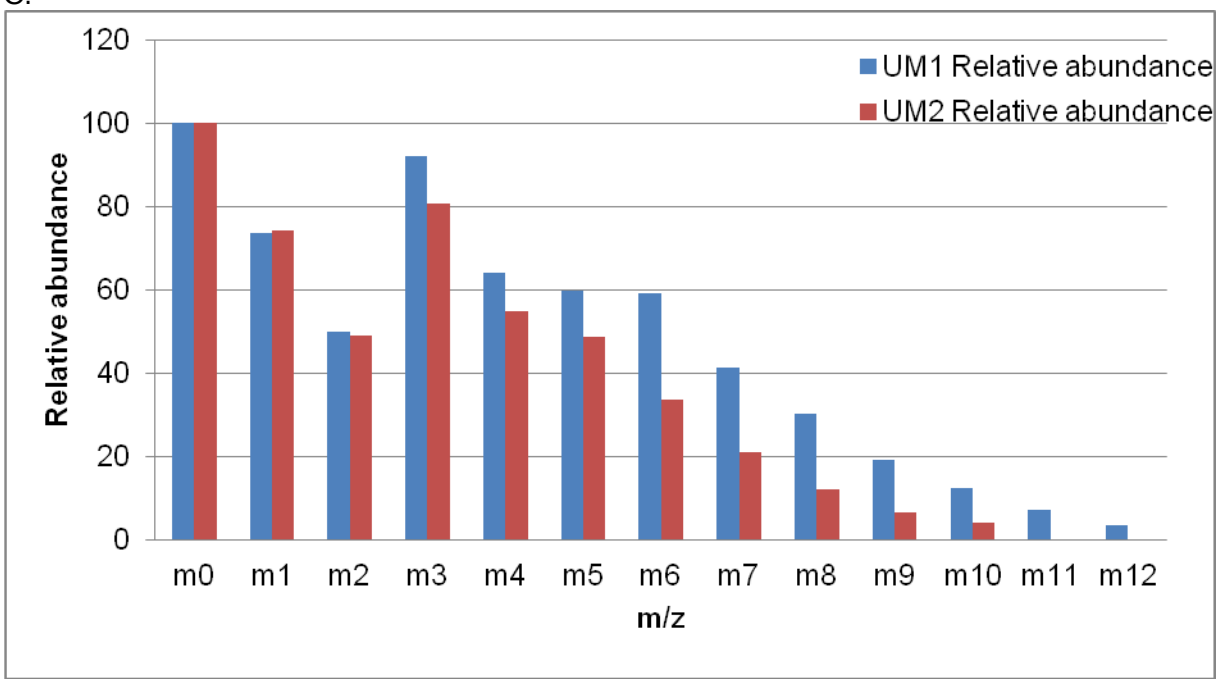

Figure 7- 3. LC-MS analysis of ^{13}C labeled peptide isotopomers in the UM1 and UM2 oral cancer cells (A) ^{13}C labeled peptide mass isotopomer distribution in UM1 oral cancer cells. (B) ^{13}C labeled peptide mass isotopomer distribution in UM2 oral cancer cells. (C) Comparison of relative abundance for ^{13}C labeled peptide mass isotopomer distribution in UM1 and UM2 oral cancer cells.

A.

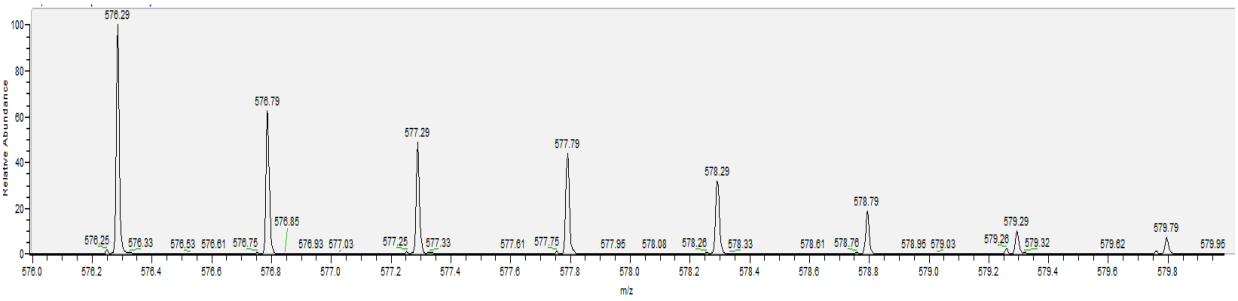

B.

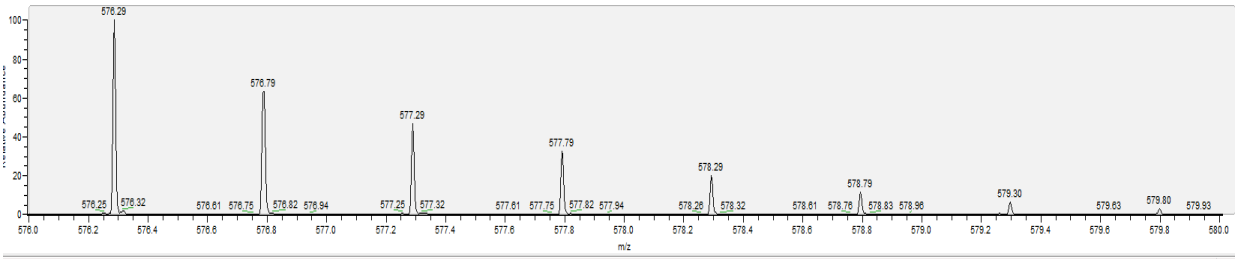

C.

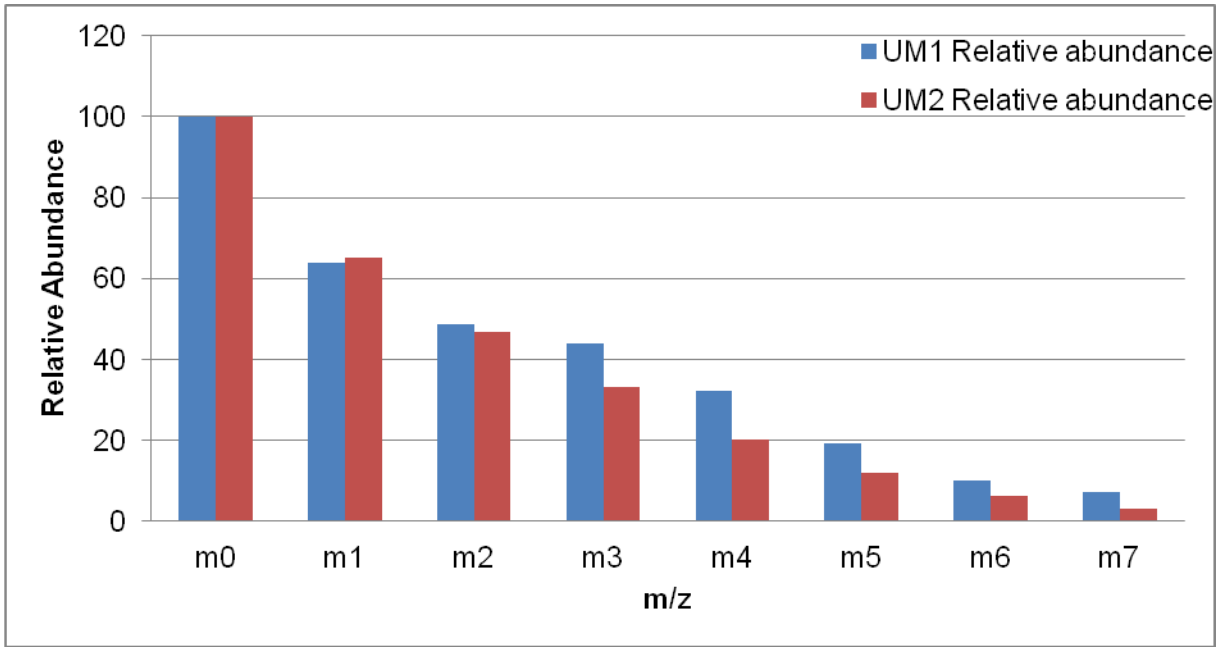

Figure 8- 1. LC-MS analysis of ^{13}C labeled peptide isotopomers in the UM1 and UM2 oral cancer cells (A) ^{13}C labeled peptide mass isotopomer distribution in UM1 oral cancer cells. (B) ^{13}C labeled peptide mass isotopomer distribution in UM2 oral cancer cells. (C) Comparison of relative abundance for ^{13}C labeled peptide mass isotopomer distribution in UM1 and UM2 oral cancer cells.

A.

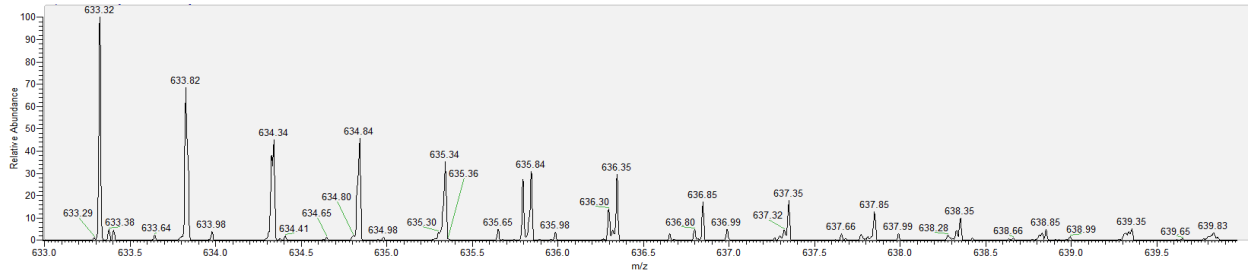

B.

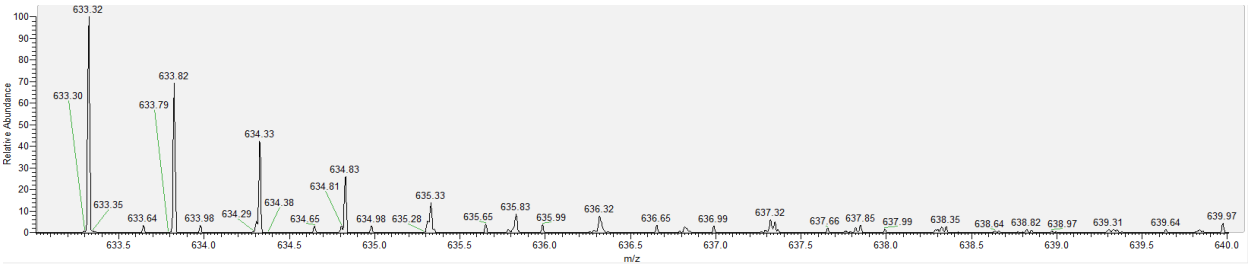

C.

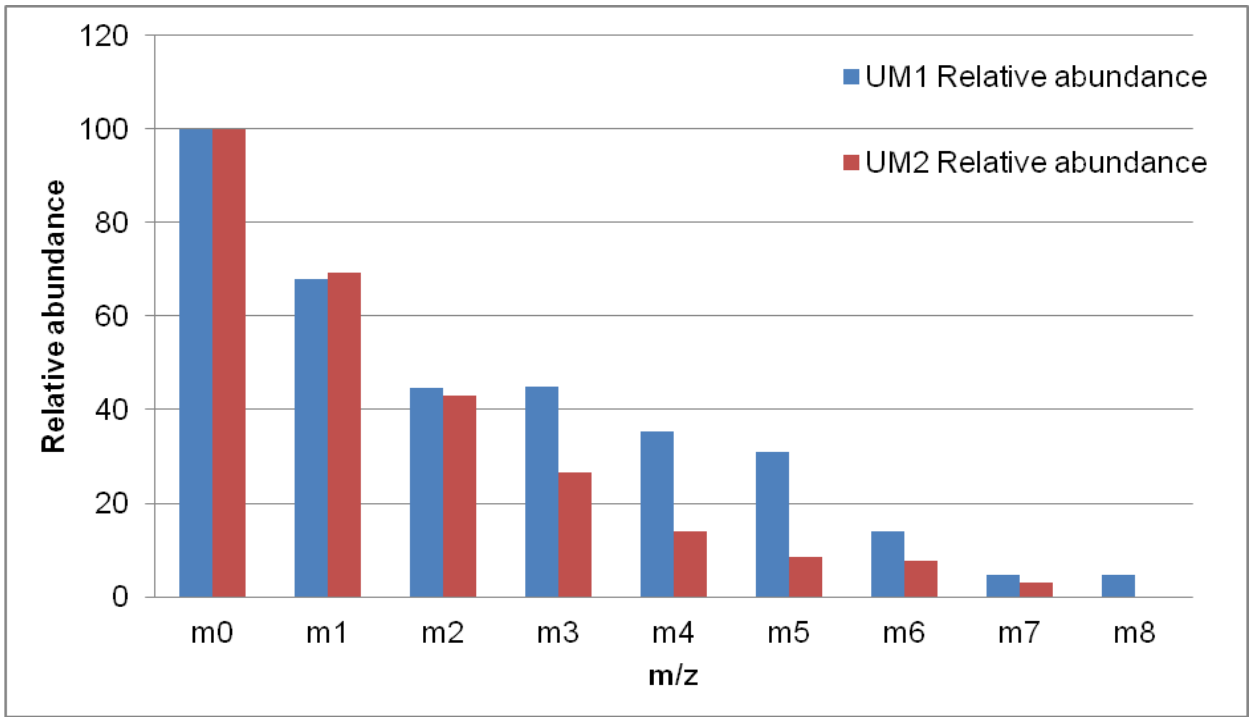

Figure 8- 2. LC-MS analysis of ^{13}C labeled peptide isotopomers in the UM1 and UM2 oral cancer cells (A) ^{13}C labeled peptide mass isotopomer distribution in UM1 oral cancer cells. (B) ^{13}C labeled peptide mass isotopomer distribution in UM2 oral cancer cells. (C) Comparison of relative abundance for ^{13}C labeled peptide mass isotopomer distribution in UM1 and UM2 oral cancer cells.

A.

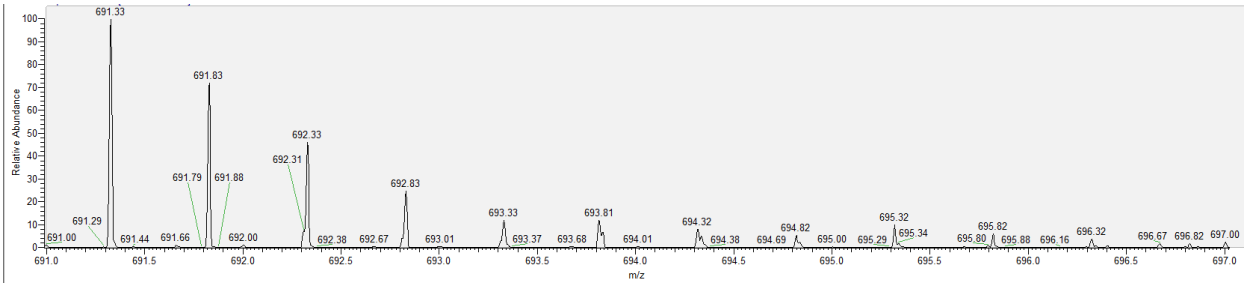

B.

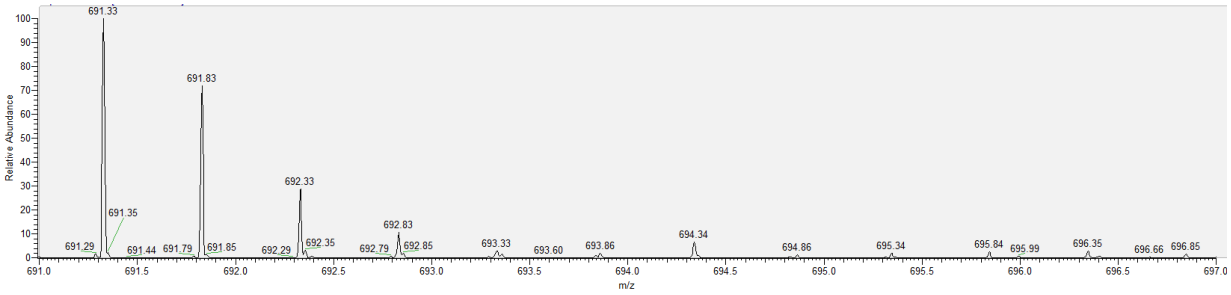

C.

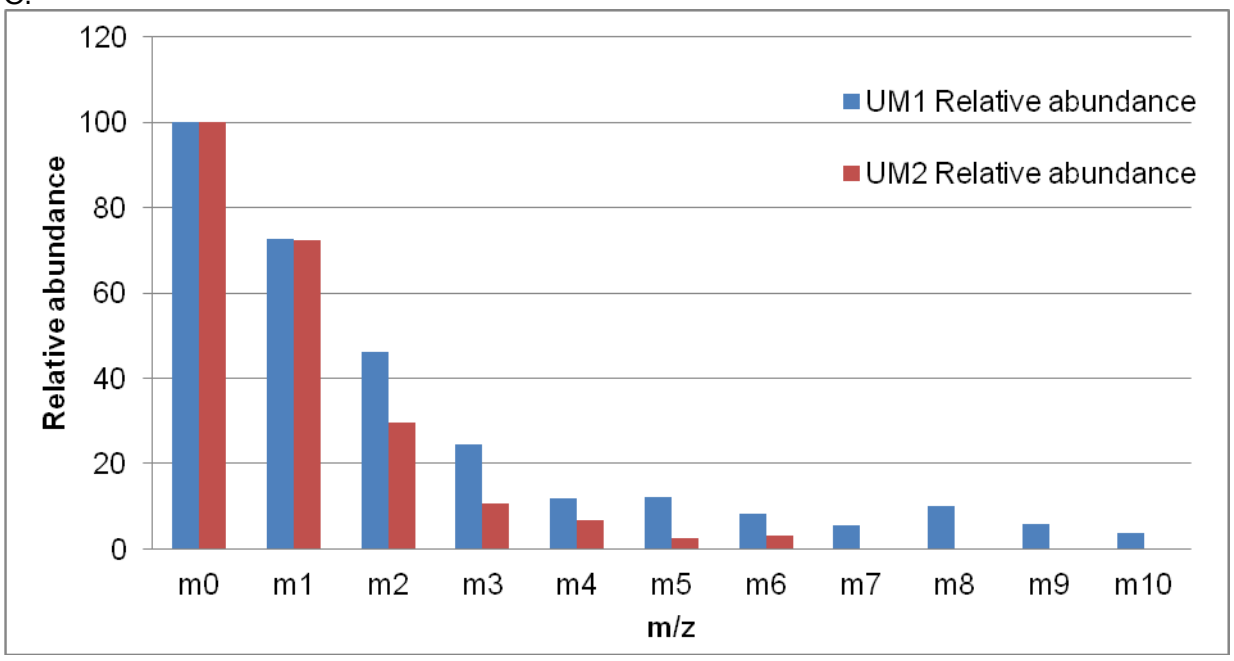

Figure 8- 3. LC-MS analysis of ^{13}C labeled peptide isotopomers in the UM1 and UM2 oral cancer cells (A) ^{13}C labeled peptide mass isotopomer distribution in UM1 oral cancer cells. (B) ^{13}C labeled peptide mass isotopomer distribution in UM2 oral cancer cells. (C) Comparison of relative abundance for ^{13}C labeled peptide mass isotopomer distribution in UM1 and UM2 oral cancer cells.

A.

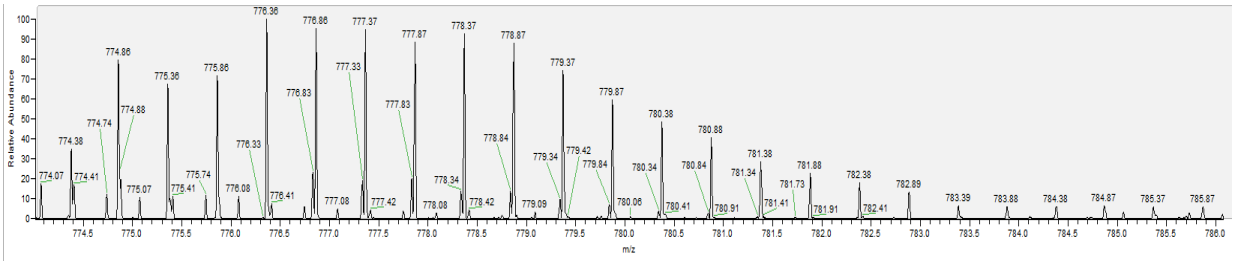

B.

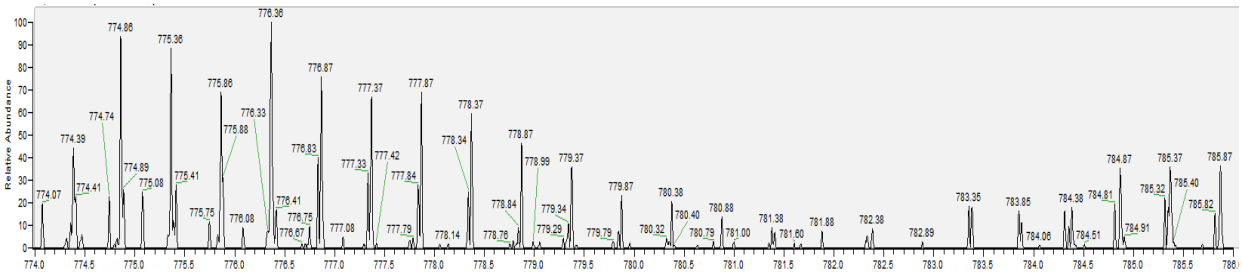

C.

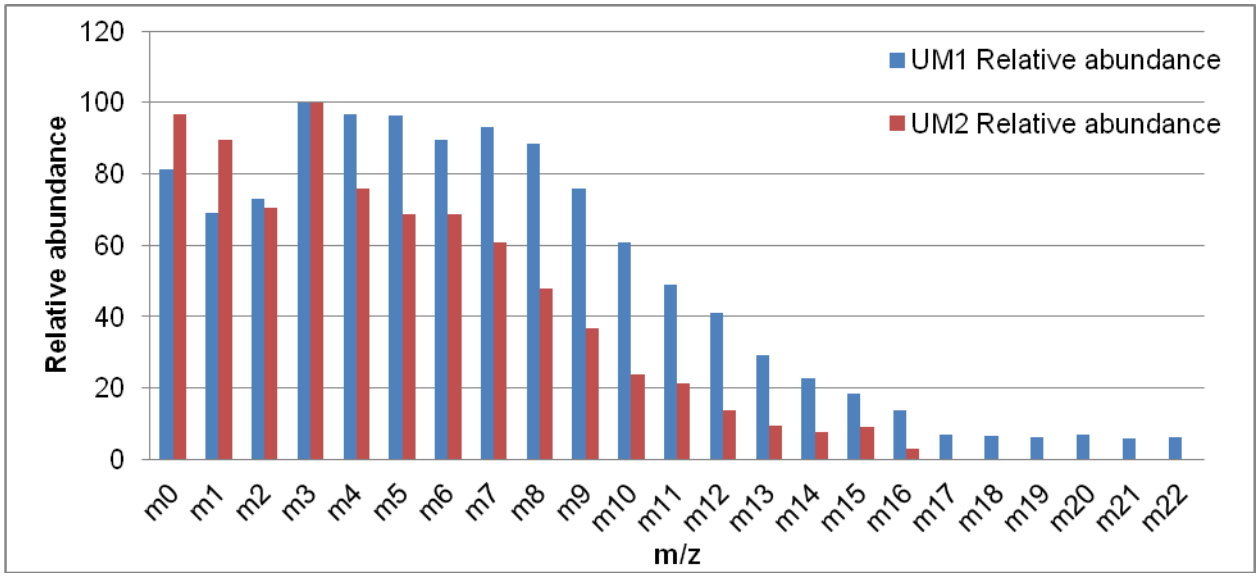

Figure 9- 1. LC-MS analysis of ^{13}C labeled peptide isotopomers in the UM1 and UM2 oral cancer cells (A) ^{13}C labeled peptide mass isotopomer distribution in UM1 oral cancer cells. (B) ^{13}C labeled peptide mass isotopomer distribution in UM2 oral cancer cells. (C) Comparison of relative abundance for ^{13}C labeled peptide mass isotopomer distribution in UM1 and UM2 oral cancer cells.

A.

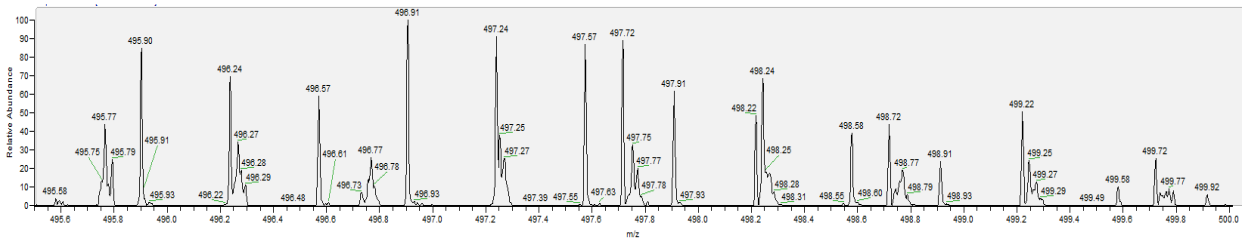

B.

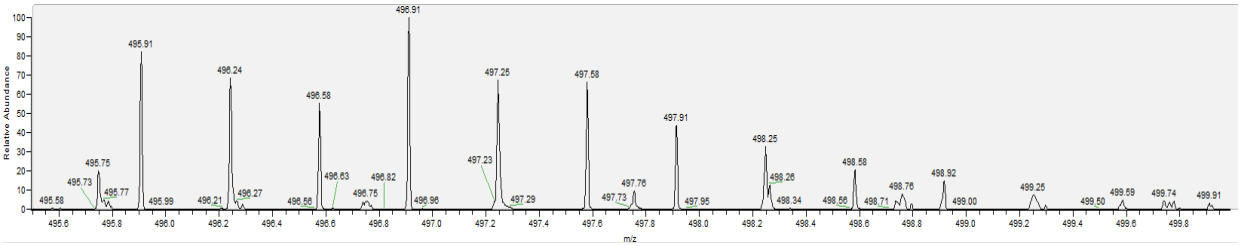

C.

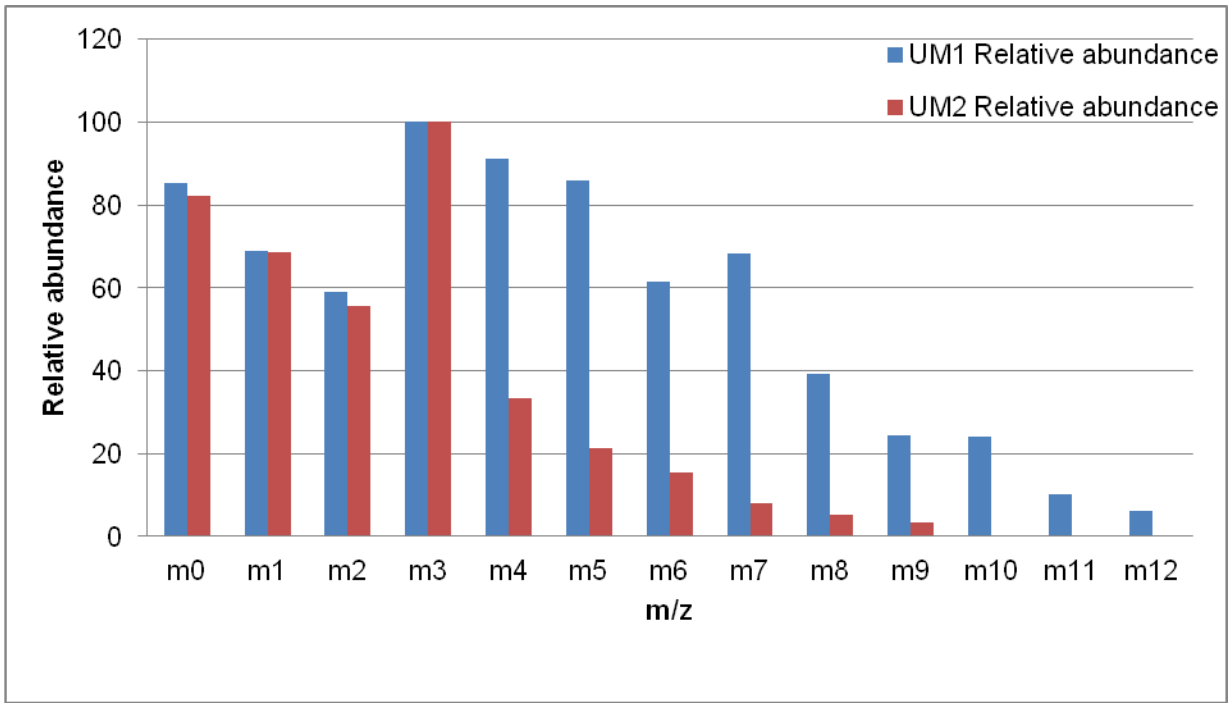

Figure 9- 2. LC-MS analysis of ^{13}C labeled peptide isotopomers in the UM1 and UM2 oral cancer cells (A) ^{13}C labeled peptide mass isotopomer distribution in UM1 oral cancer cells. (B) ^{13}C labeled peptide mass isotopomer distribution in UM2 oral cancer cells. (C) Comparison of relative abundance for ^{13}C labeled peptide mass isotopomer distribution in UM1 and UM2 oral cancer cells.

A.

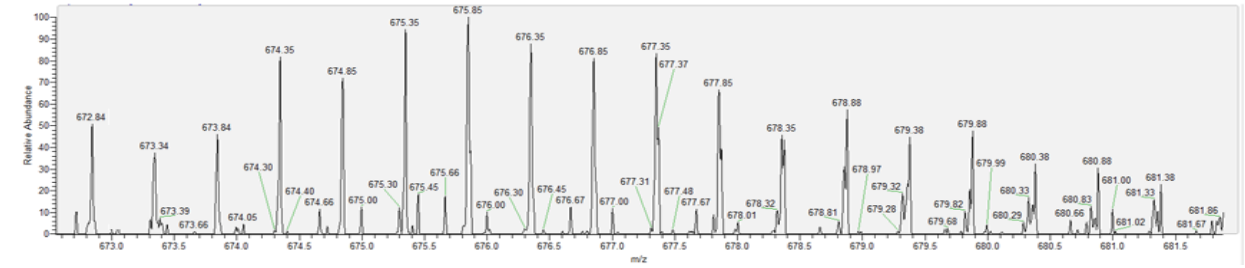

B.

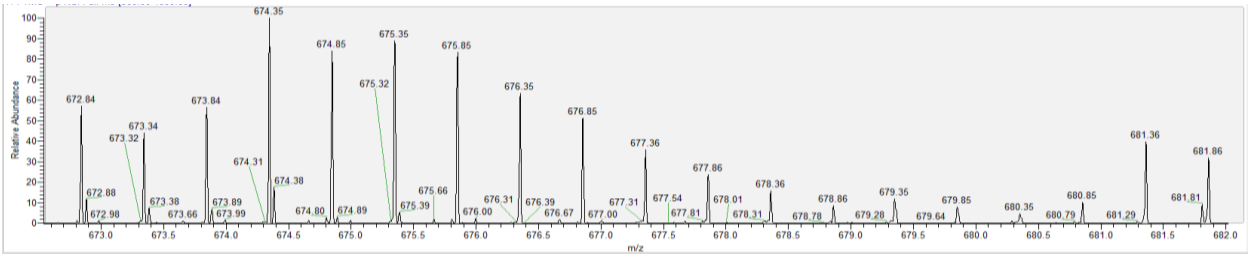

C.

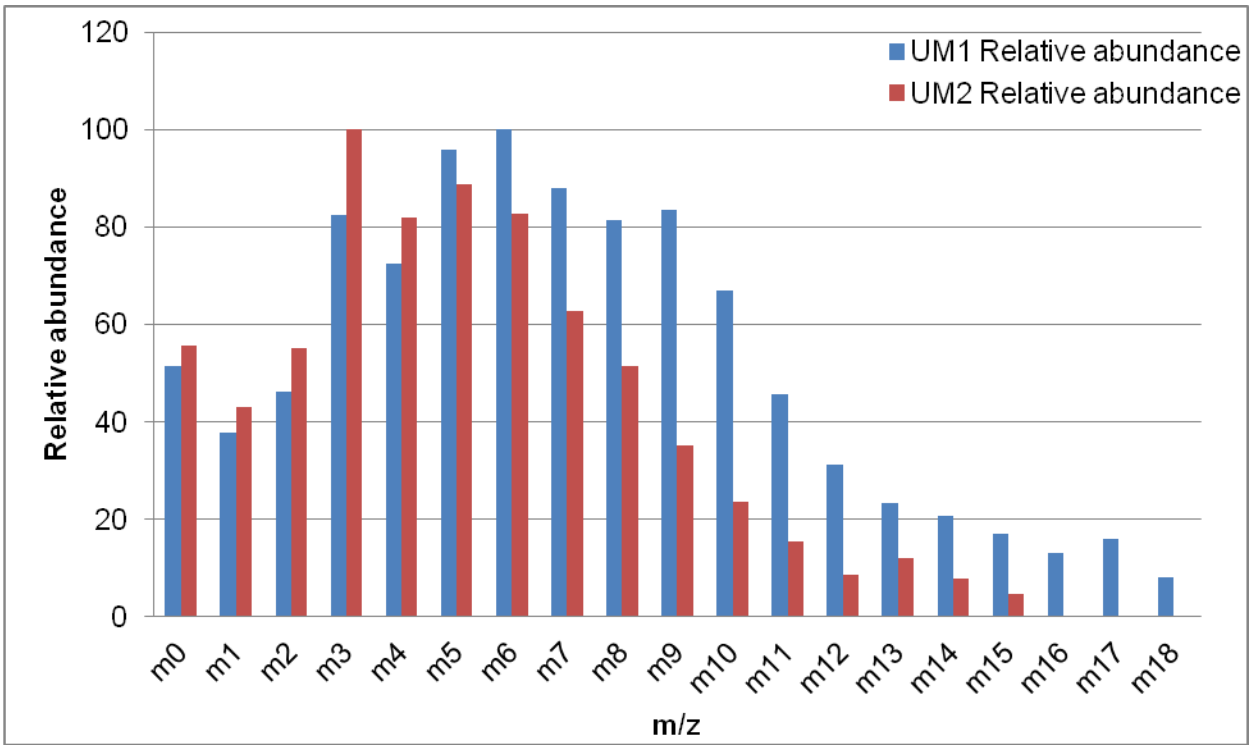

Figure 9- 3. LC-MS analysis of ^{13}C labeled peptide isotopomers in the UM1 and UM2 oral cancer cells (A) ^{13}C labeled peptide mass isotopomer distribution in UM1 oral cancer cells. (B) ^{13}C labeled peptide mass isotopomer distribution in UM2 oral cancer cells. (C) Comparison of relative abundance for ^{13}C labeled peptide mass isotopomer distribution in UM1 and UM2 oral cancer cells.

A.

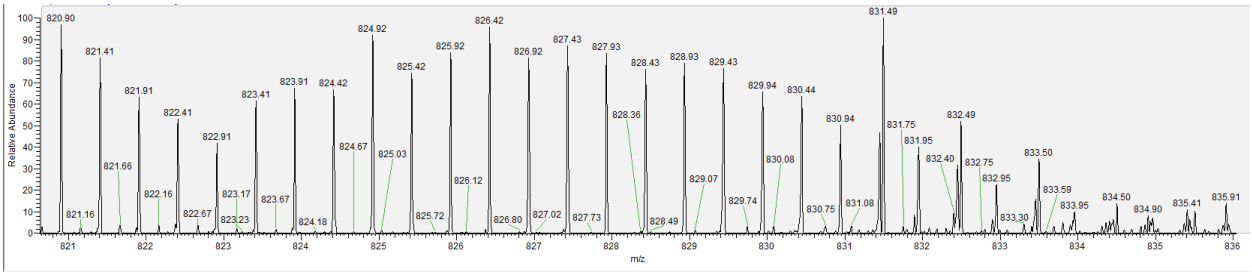

B.

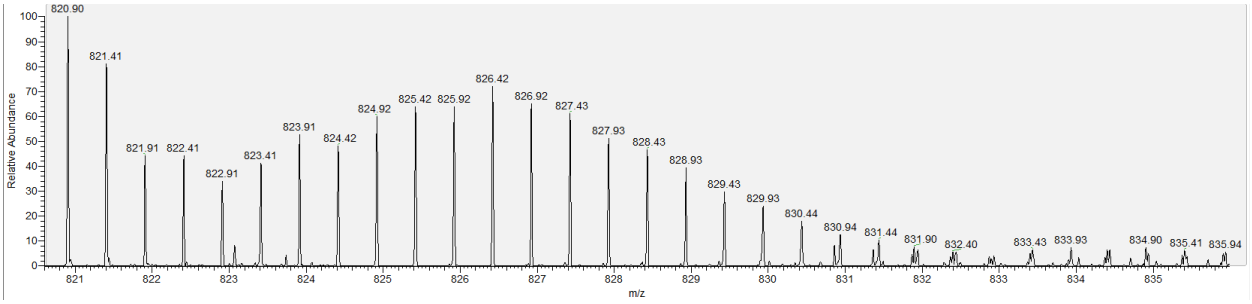

C.

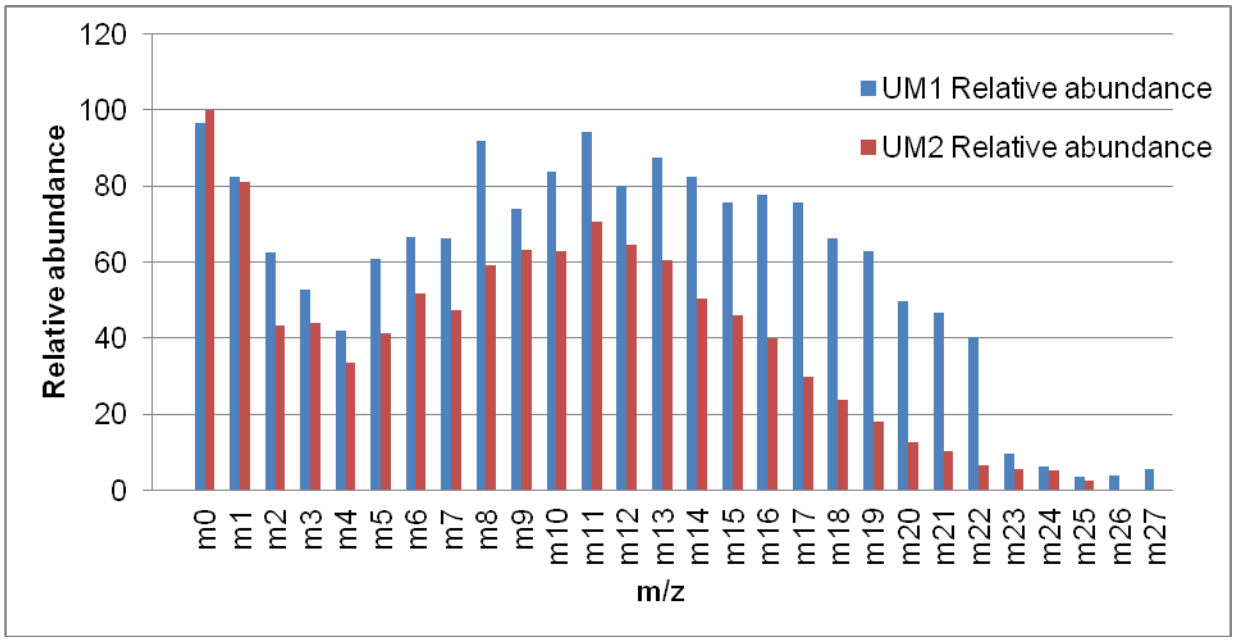

Figure 10- 1. LC-MS analysis of ^{13}C labeled peptide isotopomers in the UM1 and UM2 oral cancer cells (A) ^{13}C labeled peptide mass isotopomer distribution in UM1 oral cancer cells. (B) ^{13}C labeled peptide mass isotopomer distribution in UM2 oral cancer cells. (C) Comparison of relative abundance for ^{13}C labeled peptide mass isotopomer distribution in UM1 and UM2 oral cancer cells.

A.

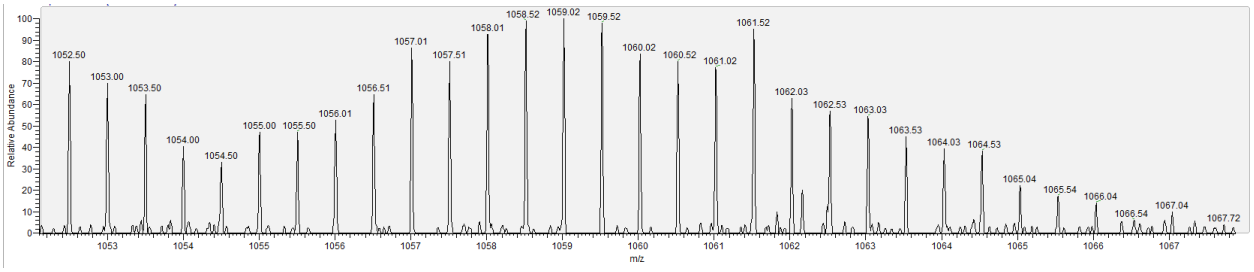

B.

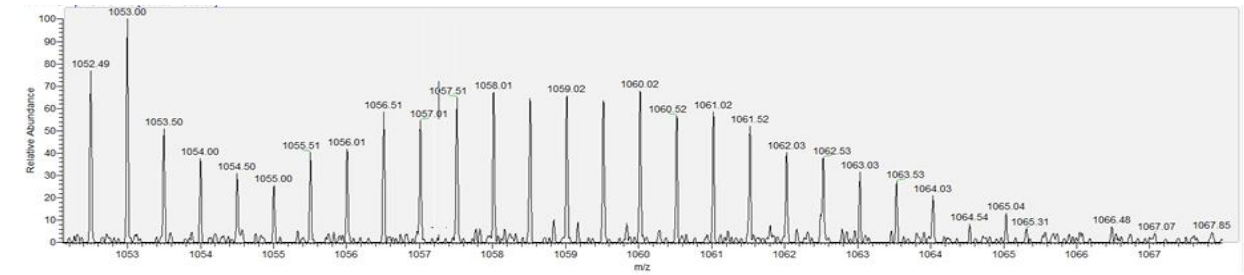

C.

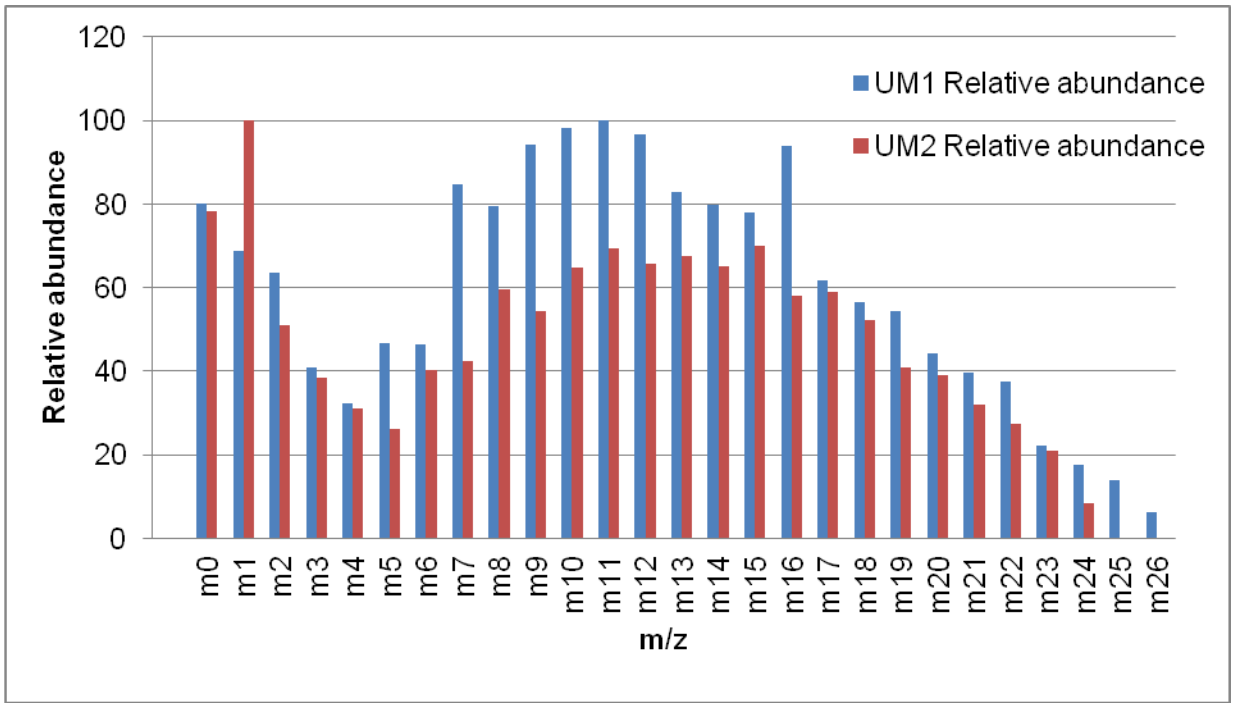

Figure 10- 2. LC-MS analysis of ^{13}C labeled peptide isotopomers in the UM1 and UM2 oral cancer cells (A) ^{13}C labeled peptide mass isotopomer distribution in UM1 oral cancer cells. (B) ^{13}C labeled peptide mass isotopomer distribution in UM2 oral cancer cells. (C) Comparison of relative abundance for ^{13}C labeled peptide mass isotopomer distribution in UM1 and UM2 oral cancer cells.

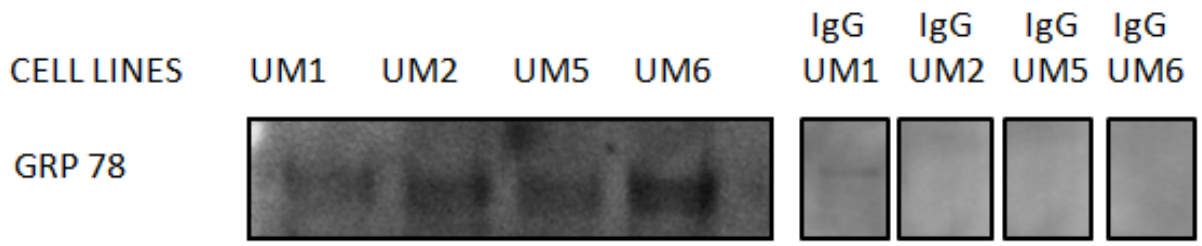

Figure 1 1. ^{13}C labeled 78kDa glucose related protein (GRP78) expression in UM1, UM2, UM5 and UM6 oral cancer cells.

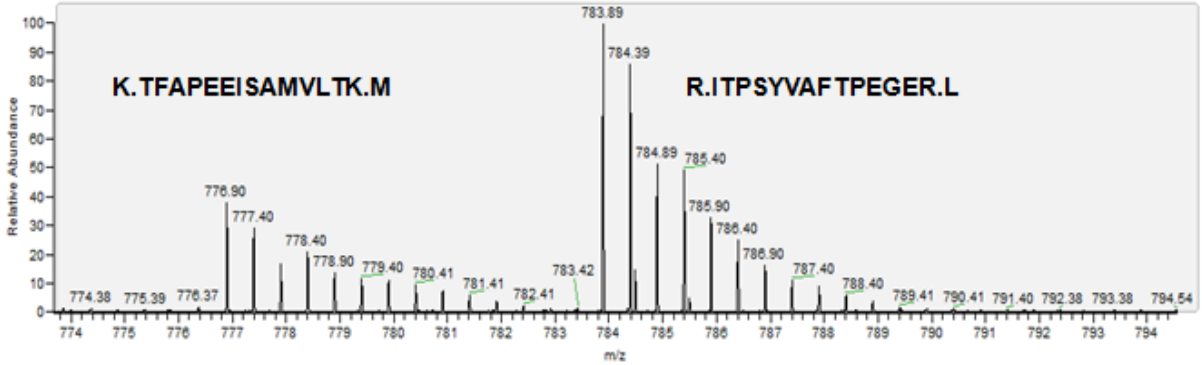

Figure 12- 1. LC- MS analysis of of ^{13}C labeled 78kDa glucose related protein (GRP78) isotopomers in UM1 oral cancer cells.

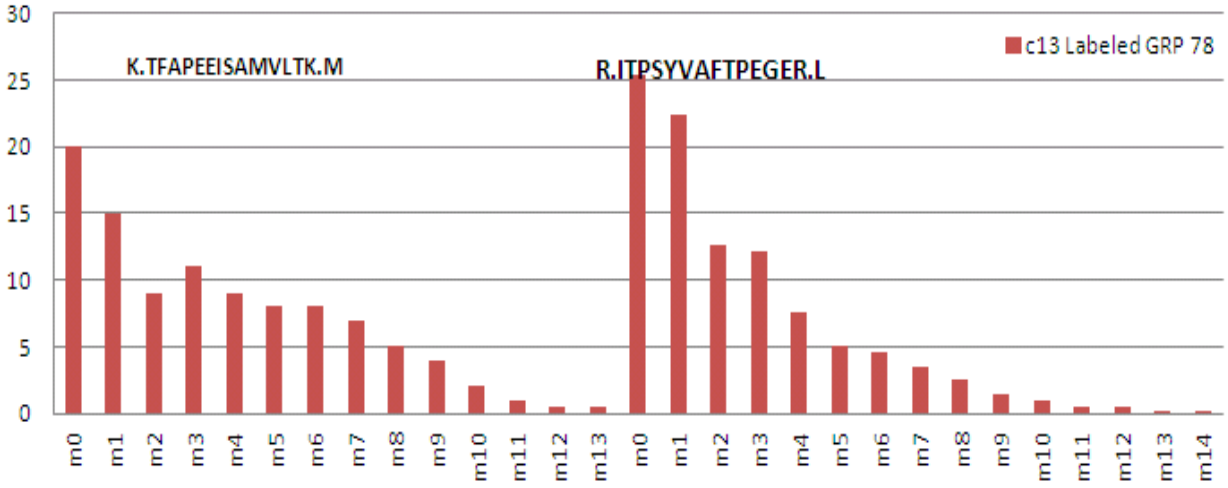

Figure 12- 2. Relative abundance for ^{13}C labeled 78kDa glucose related protein (GRP78) peptide mass isotopomer distribution in UM1 oral cancer cells.

TABLE

M766T17	M707T26	M629T19	M1265T29_1
M183T0	M802T29	M670T29	M629T19
M618T20	M172T1	M742T29	M742T29
M654T29_1	M783T29_2	M616T14	M616T14
M249T19_1	M249T19_1	M767T29_1	M707T29_2
M707T26	M709T29	M766T17	M604T15
M587T15	M587T15	M249T19_1	M767T29_1
M802T29	M586T15	M918T29	M709T29_2
M586T15	M630T15	M901T29_2	M766T17
M519T29	M604T15	M368T19	M708T29_2
M604T15	M648T15	M367T19	M1265T29_2
M709T29	M709T25	M903T29_2	M710T29
M412T19	M766T17	M708T29_2	M412T19
M537T29	M602T14	M321T19	M586T15
M602T14	M631T15	M707T29_2	M902T29_1
M893T26	M706T27	M604T15	M901T29_2
M783T29_2	M183T0	M384T19_1	M670T29
M648T15	M519T29	M385T19	M602T14
M709T25	M398T19_1	M772T9_1	M918T29
M706T27	M385T19	M728T29_1	M249T19_1
M631T15	M412T19	M771T9_1	M274T29_1

M321T19	M343T25	M709T29_2	M367T19
M343T25	M893T26	M406T19	M321T19
M367T19	M406T19	M425T19	M389T23
M398T19_1	M537T29	M398T19_1	M384T19_1
M172T1	M367T19	M389T23	M728T29_1
M385T19	M292T24_1	M710T29	M398T19_1
M630T15	M389T23	M412T19	M385T19
M389T23	M405T19	M391T19	M391T19
M406T19	M321T19	M1265T29_2	M406T19
M405T19	M390T19	M586T15	M158T19
M705T25	M389T19	M405T19	M664T30
M390T19	M279T21_2	M455T19_2	M405T19
M264T16	M289T17_2	M902T29_1	M425T19
M389T19	M268T17	M841T29_2	M390T23
M425T19_2	M183T1_2	M389T19	M455T19_2
M101T19	M425T19_2	M390T19	M390T19
M279T21_2	M183T1_1	M390T23	M389T19
M364T27	M101T19	M158T19	M771T9_1
M268T17	M390T23	M697T17	M368T19
M292T24_1	M289T17_1	M602T14	M630T15
M697T17	M533T21_1	M201T17_1	M793T9_1
M218T17	M140T17	M238T20	M697T17
M390T23	M426T17	M252T19_1	M772T9_1
M183T1_2	M264T16	M289T17_2	M201T17_1
M183T1_1	M291T17	M290T17	M252T19_1

M291T17	M697T17	M696T17	M238T20
M289T17_2	M218T17	M386T9_2	M290T17
M533T21_1	M555T21	M269T17	M289T17_2
M140T17	M556T21_2	M312T21	M269T17
M555T21	M197T20	M533T21	M255T17
M556T21_2	M155T21	M297T20	M696T17
M426T17	M298T21_1	M267T21_2	M297T20
M701T17	M269T21	M267T21_3	M533T21
M155T21	M701T17	M555T21	M312T21
M158T17_1	M158T17_1	M255T17	M267T21_3
M211T21_1	M354T21_1	M268T21_3	M555T21
M269T21	M311T18	M99T21_1	M267T21_2
M298T21_1	M211T21_1	M211T21_1	M158T17_1
M311T18	M326T21_2	M298T21_1	M268T21_3
M354T21_1	M325T21_2	M267T21_1	M211T21_1
M197T20		M354T21_1	M267T21_1
M325T21_2		M311T18	M99T21_1
M326T21_2		M158T17_1	M311T18
		M355T21	M354T21_1
			M298T21_1
			M355T21

Table 1. Down-regulated siAK2 and PGK1 feature list among common features of metabolites between UM1 and UM2 oral cancer cells.

REFERENCES

[1] C. H. Chung, J. S. Parker, G. Karaca, J. Wu, W. K. Funkhouser, D. Moore, D. Butterfoss, D. Xiang, A. Zanation, X. Yin, W. W. Shockley, M. C. Weissler, L. G. Dressler, C. G. Shores, W. G. Yarbrough, and C. M. Perou, "Molecular classification of head and neck squamous cell carcinomas using patterns of gene expression.," *Cancer Cell*, vol. 5, no. 5, pp. 489–500, May 2004.

[2] P. C. Deaths, "Cancer Statistics , 2011 The Impact of Eliminating Socioeconomic and Racial Disparities on Premature Cancer Deaths," 2011.

[3] M. E. Arellano-Garcia, R. Li, X. Liu, Y. Xie, X. Yan, J. a Loo, and S. Hu, "Identification of tetranectin as a potential biomarker for metastatic oral cancer.," *Int. J. Mol. Sci.*, vol. 11, no. 9, pp. 3106–21, Jan. 2010.

[4] M. Surgery and D. Sciences, "THE E-CADHERIN GENE IS SILENCED BY CpG METHYLATION IN HUMAN," vol. 673, no. May, pp. 667–673, 2001.

[5] S. Hu, T. Yu, Y. Xie, Y. Yang, Y. Li, X. Zhou, S. Tsung, R. R. Loo, J. R. Loo, and D. T. Wong, "Discovery of oral fluid biomarkers for human oral cancer by mass spectrometry.," *Cancer Genomics Proteomics*, vol. 4, no. 2, pp. 55–64, 2007.

[6] G. G. Xiao, R. R. Recker, and H.-W. Deng, "Recent advances in proteomics and cancer biomarker discovery.," *Clin. Med. Oncol.*, vol. 2, no. 402, pp. 63–72, Jan. 2008.

[7] V. H. Wysocki, K. A. Resing, Q. Zhang, and G. Cheng, "Mass spectrometry of peptides and proteins," vol. 35, pp. 211–222, 2005.

[8] D. Lin, D. L. Tabb, and J. R. Yates, "Large-scale protein identification using mass spectrometry," vol. 1646, pp. 1–10, 2003.

[9] P. L. Wood, "Mass spectrometry strategies for clinical metabolomics and lipidomics in psychiatry, neurology, and neuro-oncology.," *Neuropsychopharmacology*, vol. 39, no. 1, pp. 24–33, Jan. 2014.

[10] K. Dettmer, P. A. Aronov, and B. D. Hammock, "MASS SPECTROMETRY-BASED METABOLOMICS," pp. 51–78, 2007.

[11] R. Tautenhahn, K. Cho, W. Uritboonthai, Z. Zhu, G. J. Patti, and G. Siuzdak, "An accelerated workflow for untargeted metabolomics using the METLIN database.," *Nat. Biotechnol.*, vol. 30, no. 9, pp. 826–8, Sep. 2012.

[12] G. J. Patti, R. Tautenhahn, D. Rinehart, K. Cho, L. P. Shriver, M. Manchester, I. Nikolskiy, C. H. Johnson, N. G. Mahieu, and G. Siuzdak, "A view from above: cloud plots to visualize global metabolomic data.," *Anal. Chem.*, vol. 85, no. 2, pp. 798–804, Jan. 2013.

[13] R. Tautenhahn, G. J. Patti, D. Rinehart, and G. Siuzdak, “XCMS Online: a web-based platform to process untargeted metabolomic data.,” *Anal. Chem.*, vol. 84, no. 11, pp. 5035–9, Jun. 2012.

[14] J. Wang, T. T. Christison, K. Misuno, L. Lopez, A. F. Huhmer, Y. Huang, and S. Hu, “Metabolomic Pro fi ling of Anionic Metabolites in Head and Neck Cancer Cells by Capillary Ion Chromatography with Orbitrap Mass Spectrometry,” 2014.

[15] P. Dzeja and A. Terzic, “Adenylate kinase and AMP signaling networks: metabolic monitoring, signal communication and body energy sensing.,” *Int. J. Mol. Sci.*, vol. 10, no. 4, pp. 1729–72, May 2009.

[16] J. Wang, G. Ying, J. Wang, Y. Jung, J. Lu, J. Zhu, K. J. Pienta, and R. S. Taichman, “Characterization of phosphoglycerate kinase-1 expression of stromal cells derived from tumor microenvironment in prostate cancer progression.,” *Cancer Res.*, vol. 70, no. 2, pp. 471–80, Jan. 2010.

[17] S. S. S. Ahmad, J. Glatzle, K. Bajaeifer, S. Bühler, T. Lehmann, I. Königsrainer, J. Vollmer, B. Sipos, H. Northoff, A. Königsrainer, and D. Zieker, “Phosphoglycerate kinase 1 as a promoter of metastasis in colon cancer.,” *Int. J. Oncol.*, vol. 43, no. 2, pp. 586–90, Aug. 2013.

[18] K. Misuno, X. Liu, S. Feng, and S. Hu, “Quantitative proteomic analysis of sphere-forming stem-like oral cancer cells.,” *Stem Cell Res. Ther.*, vol. 4, no. 6, p. 156, Dec. 2013.

[19] A. Rasola, L. Neckers, and D. Picard, “Mitochondrial oxidative phosphorylation TRAP(1)ped in tumor cells,” *Trends Cell Biol.*, no. 1, pp. 1–9, Apr. 2014.

[20] M. Zhang, Y. D. Chai, J. Brumbaugh, X. Liu, R. Rabii, S. Feng, K. Misuno, D. Messadi, and S. Hu, “Oral cancer cells may rewire alternative metabolic pathways to survive from siRNA silencing of metabolic enzymes.,” *BMC Cancer*, vol. 14, no. 1, p. 223, Jan. 2014.

[21] J. Ai, H. Huang, X. Lv, Z. Tang, T. Chen, W. Duan, H. Sun, Q. Li, Y. Liu, J. Duan, Y. Yang, Y. Wei, and Y. Li, “Cellular Physiology and Biochemistr y Biochemistry FLNA and PGK1 are Two Potential Markers for Progression in Hepatocellular Carcinoma,” *Cell. Physiol. Biochem.*, vol. 27, no. 2011, pp. 207–216, 2011.

[22] J. Wang, J. Wang, J. Dai, Y. Jung, C.-L. Wei, Y. Wang, A. M. Havens, P. J. Hogg, E. T. Keller, K. J. Pienta, J. E. Nor, C.-Y. Wang, and R. S. Taichman, “A glycolytic mechanism regulating an angiogenic switch in prostate cancer.,” *Cancer Res.*, vol. 67, no. 1, pp. 149–59, Jan. 2007.

[23] A. Schulze and A. L. Harris, “How cancer metabolism is tuned for proliferation and vulnerable to disruption.,” *Nature*, vol. 491, no. 7424, pp. 364–73, Nov. 2012.

[24] C. a Smith, E. J. Want, G. O’Maille, R. Abagyan, and G. Siuzdak, “XCMS: processing mass spectrometry data for metabolite profiling using nonlinear peak alignment, matching, and identification.,” *Anal. Chem.*, vol. 78, no. 3, pp. 779–87, Feb. 2006.

[25] M. G. Vander Heiden, L. C. Cantley, and C. B. Thompson, “Understanding the Warburg effect: the metabolic requirements of cell proliferation.,” *Science*, vol. 324, no. 5930, pp. 1029–33, May 2009.

[26] Y. D. Chai, “Proteomic analysis of cancer cell metabolism,” *ProQuest Diss. These*, p. 170, 2013.

[27] N. I. T. Metabolomics, “International Conference on Diet , Nutrition , and Cancer,” pp. 3027–3032, 2005.

[28] W.-N. Paul Lee, P. N. Wahjudi, J. Xu, and V. L. Go, “Tracer-based metabolomics: concepts and practices.,” *Clin. Biochem.*, vol. 43, no. 16–17, pp. 1269–77, Nov. 2010.

[29] G. G. Xiao, M. Garg, S. Lim, D. Wong, V. L. Go, and W.-N. P. Lee, “Determination of protein synthesis in vivo using labeling from deuterated water and analysis of MALDI-TOF spectrum.,” *J. Appl. Physiol.*, vol. 104, no. 3, pp. 828–36, Mar. 2008.

[30] B. Turriziani, A. Garcia-Munoz, R. Pilkington, C. Raso, W. Kolch, and A. von Kriegsheim, “On-Beads Digestion in Conjunction with Data-Dependent Mass Spectrometry: A Shortcut to Quantitative and Dynamic Interaction Proteomics,” *Biology (Basel).*, vol. 3, no. 2, pp. 320–332, Apr. 2014.

[31] M. Zhang, Y. D. Chai, J. Brumbaugh, X. Liu, R. Rabii, S. Feng, K. Misuno, D. Messadi, and S. Hu, “Oral cancer cells may rewire alternative metabolic pathways to survive from siRNA silencing of metabolic enzymes.,” *BMC Cancer*, vol. 14, no. 1, p. 223, Jan. 2014.

[32] Q. Zhang, N. P. Botting, and C. Kay, “A gram scale synthesis of a multi-13C-labelled anthocyanin, [6,8,10,3’,5'-13C5]cyanidin-3-glucoside, for use in oral tracer studies in humans.,” *Chem. Commun. (Camb).*, vol. 47, no. 38, pp. 10596–8, Oct. 2011.